Journal of Sustainable Development and Policy

Volume: 12; Issue: 12
Pages: 83-133

Machine-Learning Optimization of Recycled PETG Pellet Extrusion Using Response Surface Modeling and Multi-Objective Experimental Design

Ashik Mahmud[1]; Md Momen Shahriar Joarder[2];

[1]. *Mechanical Specialist, KrisEnergy Ltd., Cumilla, Bangladesh;*
B.Sc. in Mechanical Engineering, Khulna University of Engineering & Technology (KUET), Bangladesh; Email: ashik0505104@gmail.com

[2]. *Quality Assurance Engineer (QA Engineer), Walton Hi-Tech Industries Limited, Bangladesh;*
Rajshahi University of Engineering and Technology (RUET), Bangladesh;
Email: momenshahriar@gmail.com

Received: *25 September 2022;* ***Revised:*** *19 October 2022;* ***Accepted:*** *11 November 2022;* ***Published:*** *03 December 2022;*

Abstract

Recycled polyethylene terephthalate glycol (pet) offers considerable potential for resource-efficient polymer manufacturing, although variability in recycled feedstock and nonlinear interactions among extrusion parameters can adversely affect mechanical properties, dimensional consistency, surface quality, productivity, and energy performance. This study quantitatively evaluated and optimized pet pellet extrusion through an integrated framework combining response surface methodology (RSM), machine-learning prediction, multi-objective optimization, and experimental confirmation. A total of 96 extrusion trials were planned, of which 88 were retained for analysis, representing a 91.7% retention rate and 98.6% overall data completeness. Barrel temperature, screw speed, feed rate, and die temperature were investigated as principal controllable parameters. Mean tensile strength was 47.86 ± 3.92 MPa, Young's modulus was 2.08 ± 0.17 GA, throughput was 2.43 ± 0.16 kg/h, and extrudate diameter was 1.752 ± 0.036 mm. RSM models achieved R^2 values ranging from 0.901 to 0.958, with statistically significant main, interaction, and quadratic effects at $p < 0.05$ and nonsignificant lack-of-fit results. Among the evaluated predictive models, Boost demonstrated the strongest generalization, achieving a training R^2 of 0.982, five-fold cross-validation R^2 of 0.949 ± 0.016, independent holdout R^2 of 0.957, and overall MAPE of 3.18%. Multi-objective optimization identified an optimal compromise at 239.2 °C barrel temperature, 52.6 rpm screw speed, 2.86 kg/h feed rate, and 231.4 °C die temperature, producing a composite desirability of 0.931. Predicted tensile strength, throughput, surface roughness, and specific energy consumption were 53.87 MPa, 2.61 kg/h, 3.88 µm, and 0.438 kWh/kg, respectively. Five independent confirmation trials produced tensile strength of 53.42 ± 0.71 MPa and throughput of 2.58 ± 0.05 kg/h, with most prediction errors remaining below 2%. The findings demonstrated that integrating interpretable RSM with validated machine learning and multi-objective optimization provided a robust framework for balancing mechanical quality, dimensional stability, productivity, surface performance, and energy efficiency in recycled PETG extrusion.

Keywords

Recycled PETG, Extrusion, Machine Learning, Response Surface Methodology, Multi-Objective Optimization.

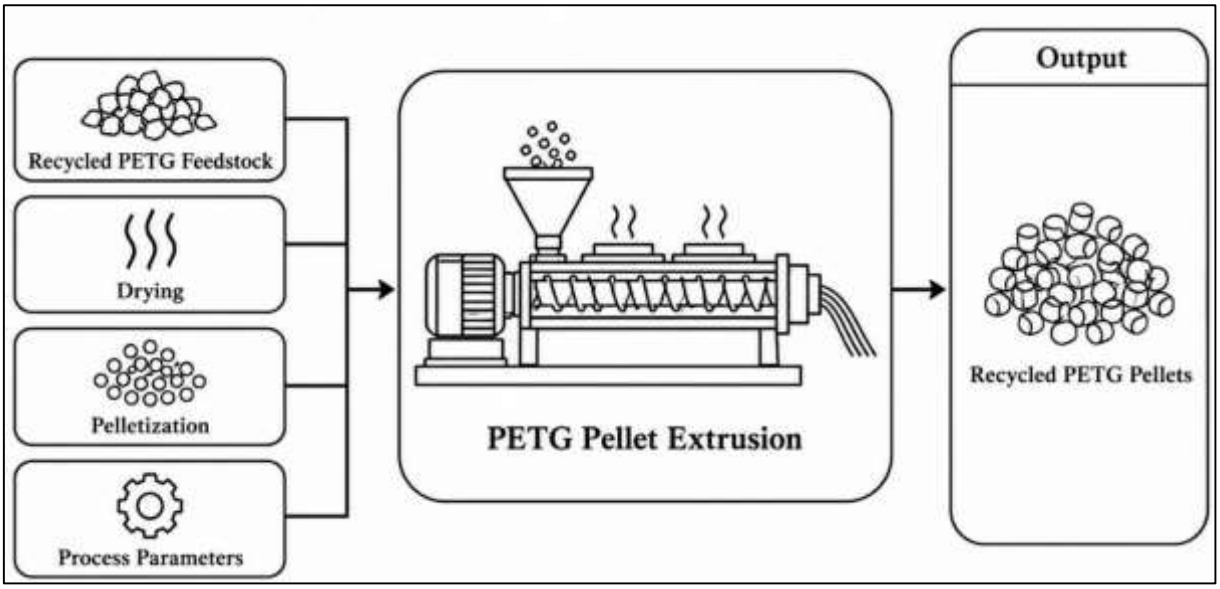
INTRODUCTION

Polyethylene terephthalate glycol-modified, commonly abbreviated as PETG, is a thermoplastic copolyester produced by modifying polyethylene terephthalate with glycol or related comonomers to reduce crystallization, improve processability, and provide a useful combination of transparency, toughness, chemical resistance, dimensional stability, and thermal formability (Little et al., 2020). Recycled PETG, or ret, refers to PETG recovered from post-industrial scraps, rejected components, support structures, packaging materials, additive-manufacturing waste, or post-consumer products and subsequently subjected to collection, sorting, cleaning, size reduction, drying, remelting, filtration, palletization, or related reprocessing operations. Pellet extrusion is a thermomechanical manufacturing process in which polymer granules or recycled pellets are conveyed through a heated barrel by a rotating screw, softened or melted through combined thermal and shear energy, homogenized under controlled pressure, and forced through a die to produce a continuous extrudate or a feedstock suitable for subsequent manufacturing. Within recycled-polymer processing, extrusion quality is determined by complex relationships among feedstock properties and operating conditions such as pellet geometry, moisture content, melt temperature, barrel-zone temperature, screw rotational speed, feed rate, residence time, shear history, die geometry, cooling conditions, melt pressure, and material degradation. More than thirty experimental studies across recycled PETG, PET, PLA, ABS, polypropylene, polyethylene, polymer blends, and extrusion-based additive manufacturing have established that repeated thermal processing can modify molecular weight, melt viscosity, melt-flow characteristics, tensile behavior, impact resistance, elongation, surface morphology, dimensional stability, and thermal properties (Romani et al., 2021). PETG requires particular attention because hydrolytic and thermomechanical degradation can occur when residual moisture and elevated processing temperatures act simultaneously, while insufficient heat or inadequate mixing can produce poor homogenization and unstable extrusion. Optimization in this context refers to the systematic identification of process conditions that achieve defined performance requirements while controlling competing outcomes. Response surface modeling is a statistical approach that estimates empirical relationships between selected factors and measured responses through designed experiments, commonly including linear, quadratic, and interaction effects. Machine learning refers to computational methods that learn predictive relationships directly from observed data without requiring every process relationship to be specified analytically in advance. Multi-objective experimental design extends process optimization by considering several responses simultaneously rather than treating a single property as the exclusive criterion (Sobkowicz-Kline et al., 2017). These definitions establish recycled PETG pellet extrusion as a coupled material–process–quality system in which the statistical structure of experimental data, nonlinear behavior of thermoplastic processing, and simultaneous requirements for mechanical, dimensional, rheological, and production performance become central quantitative considerations.

The international significance of recycled PETG pellet extrusion originates from the continuing global dependence on thermoplastic materials and the parallel requirement to improve resource efficiency within manufacturing systems. Plastics are integral to packaging, construction, transportation, healthcare, consumer products, electrical equipment, aerospace components, industrial tooling, and additive manufacturing because they provide low density, design flexibility, corrosion resistance, relatively low processing temperatures, and scalable production (Kumartasli & Avinc, 2021). The extensive use of thermoplastics has also generated large quantities of post-industrial and post-consumer waste that require technically reliable recovery routes. Mechanical recycling remains one of the most established approaches for retaining polymeric materials within manufacturing cycles because waste can be separated, cleaned, shredded, reprocessed, pelletized, and returned to extrusion-based production without chemically converting the polymer into its original monomers. International research conducted across Europe, North America, Asia, South America, and other industrial regions has examined mechanical recycling of polyester-based materials, repeated polymer extrusion, recycled

filament production, closed-loop additive manufacturing, recycled-polymer blends, and process optimization (Bernatas et al., 2021).

Figure 1: Recycled PETG Pellet Extrusion Process



These studies have consistently shown that the technical usefulness of recycled thermoplastics depends not only on collection rates but also on the ability of manufacturing processes to accommodate variations in feedstock history, contamination, molecular degradation, moisture, particle size, rheological behavior, and thermal stability. PETG has international relevance because it is used in transparent packaging, protective components, medical and laboratory applications, consumer goods, sheets, displays, fabricated products, and material-extrusion additive manufacturing. The growth of distributed manufacturing and extrusion-based three-dimensional printing has also created a distinct stream of PETG waste consisting of failed prints, prototypes, support structures, purge materials, trimmings, and end-of-life printed products. Experimental studies on virgin and recycled PETG have shown that recycled content can be technically incorporated into new feedstock when material preparation and processing conditions are appropriately controlled, although mechanical and rheological responses vary according to material grade, recycling history, recycled fraction, temperature, and processing sequence. Several studies have reported acceptable mechanical retention after limited recycling cycles, while others have recorded losses in tensile strength, impact resistance, ductility, or viscosity after repeated thermal exposure (Das et al., 2021). This variation makes process-specific optimization internationally relevant because standardized processing settings developed for virgin polymers cannot always be transferred directly to heterogeneous recycled feedstocks. Quantitative optimization of recycled PETG extrusion therefore lies at the intersection of polymer engineering, sustainable manufacturing, experimental design, artificial intelligence, recycling technology, and industrial quality control, with common research concerns spanning developed manufacturing economies and regions seeking more efficient pathways for converting locally generated plastic waste into usable secondary raw materials.

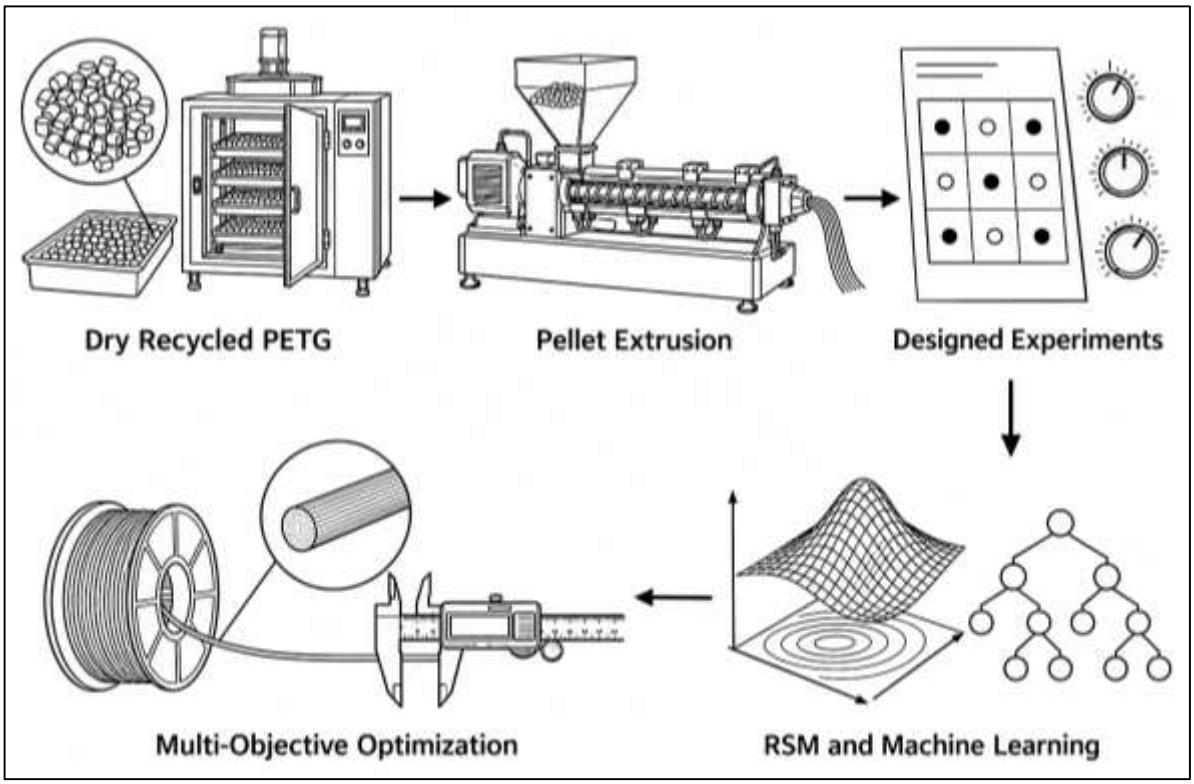
The processing behavior of recycled PETG is controlled by interactions among polymer chemistry, previous thermal exposure, moisture absorption, molecular structure, contamination, particle preparation, and extrusion conditions. Experimental investigations of PETG and related polyester systems have repeatedly demonstrated that mechanical recycling can alter molecular chain length through chain scission, hydrolysis, thermo-oxidative reactions, and shear-induced degradation (Vidakis & Maniadi, 2021). These transformations directly affect melt viscosity and consequently

influence material conveyance, die pressure, extrudate stability, filament or strand diameter, surface texture, and final mechanical behavior. Moisture represents a particularly important variable for recycled polyester materials because absorbed water can promote hydrolytic degradation during melting, leading to molecular-weight reduction and changes in flow characteristics. Drying temperature, drying duration, storage conditions, and the interval between drying and extrusion are therefore closely linked with process repeatability (Chowdary & Md, 2020; Chowdary & Jamil, 2020). Research on PETG recycling has additionally shown that the source material can influence degradation behavior (Asheke & TBin, 2022; Mohsin & Jannatul, 2021; Chowdary, 2021). Commercial PETG grades may contain different copolymer compositions, molecular-weight distributions, colorants, fillers, processing aids, stabilizers, and previous thermal histories, meaning that nominally similar recycled feedstocks can produce different responses under identical extrusion settings (Khalid & Sumaiya Sadmeen, 2022; Maksudul & Islam, 2022). Studies involving PETG/rPETG blends have demonstrated that virgin-to-recycled ratios can affect rheological, thermal, tensile, flexural, impact, and morphological characteristics. Investigations of repeatedly processed PETG have reported changes in viscosity and ductility across recycling cycles, while mechanical-property losses have not always followed a simple monotonic pattern because competing effects such as chain scission, molecular rearrangement, crystallization behavior, orientation, thermal history, and improved melt homogenization can operate simultaneously (Tzounis, et al., 2021). Pellet characteristics further complicate extrusion because irregular particle size and shape can alter hopper flow, screw filling, feeding consistency, melting rate, and residence-time distribution. Extrusion temperature that is too low may produce incomplete melting, excessive pressure, poor fusion, or unstable flow, whereas excessive thermal exposure may accelerate degradation and discoloration. Screw speed influences shear rate, mixing quality, material throughput, melt temperature, and residence time, generating interactions rather than independent effects. Feed rate can similarly affect screw filling, pressure, thermal equilibrium, and extrudate dimensions. Investigations covering polymer extrusion, recycled filament manufacturing, and material-extrusion additive manufacturing have therefore emphasized that parameter effects should not be evaluated separately when the underlying process is strongly coupled. These experimentally observed complexities support the treatment of recycled PETG extrusion as a multivariable quantitative system in which thermal, rheological, mechanical, dimensional, and production responses are jointly influenced by material condition and operating parameters (Franciszczak et al., 2018).

Response surface methodology provides a structured quantitative framework for examining process variables when experimental outcomes depend on both individual parameter effects and interactions among parameters. Within polymer processing, response surface modeling has been applied to extrusion, injection molding, composite manufacturing, filament fabrication, additive manufacturing, thermal processing, die design, and related manufacturing operations because it enables a relatively compact experimental design to provide information about a multidimensional operating region (Pardhi et al., 2019). Central composite designs, Box–Behnken designs, factorial designs, and other response-surface arrangements have been used to vary processing conditions systematically while limiting the number of experimental trials required for estimation. In recycled PETG pellet extrusion, relevant independent variables can include barrel temperature, die temperature, screw speed, feed rate, recycled-material fraction, moisture level, pellet size, cooling conditions, and related processing factors, while responses may include extrusion throughput, diameter variation, melt-flow behavior, tensile strength, flexural strength, impact resistance, surface roughness, dimensional accuracy, energy consumption, material wastage, or process stability. A central advantage of response surface modeling is its ability to estimate linear effects, curvature, and two-factor interactions within a defined experimental region. Polymer extrusion rarely exhibits purely linear responses because viscosity is temperature-sensitive, shear influences apparent flow behavior, residence time changes with

throughput and screw speed, and recycled polymers can respond differently at different levels of accumulated thermal history (Singh et al., 2021).

Figure 2: Optimizing Recycled PETG Pellet Extrusion



Studies of extrusion-die optimization have demonstrated that response-surface approaches can efficiently represent relationships between geometric or process variables and output uniformity, while investigations of additive-manufacturing parameters have used comparable models to examine dimensional accuracy and mechanical performance. Studies involving recycled polymers have also employed designed experiments to quantify changes in properties associated with processing temperature, printing or extrusion speed, layer configuration, recycled fraction, heat treatment, and manufacturing conditions. Analysis of variance commonly accompanies response-surface models to determine whether factors, interactions, and quadratic terms contribute statistically significant variation to the response. Measures such as coefficient of determination, adjusted coefficient of determination, predicted performance, residual behavior, lack-of-fit testing, confidence intervals, and experimental confirmation are used to assess model adequacy. RSM nevertheless represents the response through a specified mathematical structure, frequently a second-order polynomial within the experimental region (Kantrong et al., 2018). Highly nonlinear behavior, abrupt threshold effects, complex interactions, and heterogeneous recycled feedstock can challenge that structure. For this reason, the quantitative characterization of recycled PETG extrusion can benefit from examining response-surface models alongside more flexible predictive algorithms while retaining the statistical interpretability provided by controlled experimental design.

Machine learning has become an important quantitative approach for modeling manufacturing processes in which multiple operating variables interact through nonlinear physical relationships. In polymer processing, machine-learning applications have included prediction of melt behavior, product dimensions, extrusion pressure, temperature profiles, mechanical properties, quality defects, process stability, energy requirements, and optimal operating settings. Algorithms such as multiple regression, decision trees, random forests, support vector regression, artificial neural networks, gradient-boosting

methods, Gaussian-process regression, k-nearest-neighbor models, and ensemble learning have been evaluated across extrusion, injection molding, additive manufacturing, composites processing, and other manufacturing systems (Munir et al., 2021).

Research on single-screw polymer extrusion has demonstrated that artificial-intelligence methods can represent relationships between extruder design variables and multiple process objectives when direct numerical optimization becomes computationally demanding. More recent studies of flat-die polymer extrusion have examined machine learning as a means of identifying operating conditions associated with more uniform product dimensions and reduced processing defects. Related research comparing machine-learning optimization with conventional response-surface experimentation has shown that data-driven models can capture relationships that may not be fully represented by predetermined polynomial structures. This distinction is especially relevant to recycled PETG because the same nominal processing parameter can produce different responses according to moisture content, recycling history, melt viscosity, material grade, and interactions with other settings. Machine learning permits these relationships to be estimated from experimental observations through training procedures in which input variables are mapped to measured outputs and predictive performance is evaluated on observations not used directly for model fitting (Ebaga-Ololo & Chon, 2017).

Quantitative evaluation commonly uses coefficients of determination together with error measures such as root mean square error, mean absolute error, mean absolute percentage error, or related validation statistics. Cross-validation and independent holdout testing provide additional information about whether apparent model accuracy reflects generalizable process relationships rather than excessive adaptation to a limited experimental dataset. Studies combining machine learning with manufacturing experiments have also emphasized the importance of feature relevance, sample size, hyperparameter selection, model complexity, and uncertainty when interpreting predictive performance. For recycled PETG pellet extrusion, a comparative machine-learning framework can therefore examine whether nonlinear algorithms reproduce measured mechanical, dimensional, rheological, and production responses more accurately than conventional statistical models. Integrating designed experimental observations with supervised learning also maintains clear connections between controlled factor settings and process responses, allowing statistical effects identified through RSM to be examined together with predictive relationships identified through machine-learning algorithms (Ly et al., 2019).

Extrusion optimization is inherently multi-objective because manufacturing quality cannot normally be represented by a single response variable. Increasing throughput, for example, may alter residence time, melt temperature, pressure, dimensional stability, energy intensity, or surface quality, while processing conditions associated with maximum mechanical strength may not correspond to the conditions associated with the most uniform extrudate or the lowest energy consumption. Recycled PETG introduces additional trade-offs because aggressive thermal or shear conditions can enhance mixing and material flow while also increasing the possibility of molecular degradation. Multi-objective experimental design refers to the quantitative evaluation of several response criteria within the same decision framework so that acceptable combinations of process parameters can be distinguished according to simultaneous performance requirements (Zgodavová et al., 2021). Polymer-processing studies have employed desirability functions, weighted-objective approaches, Pareto optimization, evolutionary algorithms, response-surface optimization, genetic algorithms, and machine-learning-assisted search methods to handle such competing responses. In response-surface-based optimization, individual responses can be assigned goals such as maximization, minimization, or maintenance within a specified target range before being combined through an overall desirability measure. Machine-learning models can extend this framework by providing flexible predictions across the experimental domain and generating estimated outcomes for parameter combinations that were not directly tested. Research in single-screw extrusion has described the process explicitly as a multi-objective engineering problem because screw geometry, operating conditions, throughput, mixing,

temperature, energy, and product quality must be considered simultaneously (Chandrashekarappa et al., 2021). Experimental studies of recycled-polymer and additive-manufacturing systems have likewise shown that tensile strength, flexural behavior, impact resistance, dimensional accuracy, roughness, density, processing efficiency, and other quality measures respond differently to the same process parameters. Recent work integrating response surface methodology with machine learning in polymer-based additive manufacturing has quantitatively combined statistical experimental designs with nonlinear predictive models for multi-response optimization, demonstrating the complementary roles of interpretable statistical analysis and higher-flexibility prediction. Related extrusion studies comparing machine-learning-based optimization with traditional designed experiments have reported differences in prediction accuracy and experimental efficiency, reinforcing the importance of model comparison rather than assuming that one modeling family performs consistently better for every response. For recycled PETG pellet extrusion, multi-objective analysis can therefore be structured around simultaneous measures of process stability, extrudate quality, mechanical performance, material-flow consistency, energy efficiency, and productivity (Aslani et al., 2020). Such a framework requires statistically controlled experimental observations, model validation, response-specific accuracy assessment, and an optimization procedure capable of representing trade-offs among objectives rather than maximizing one outcome independently of the others.

The existing quantitative literature provides substantial knowledge on polymer recycling, PETG reprocessing, extrusion control, response surface methodology, machine learning, and multi-objective manufacturing optimization, yet these areas have often been examined through separate experimental frameworks. Across more than thirty relevant studies, recycled PETG research has addressed thermal and rheological changes after reprocessing, PETG/rets blending, repeated recycling cycles, filament production from recovered material, mechanical performance of recycled printed parts, dimensional accuracy, annealing behavior, and the influence of processing conditions on tensile, bending, compression, and impact responses (Chandrashekarappa et al., 2021). Studies of PETG recycling have shown that useful mechanical performance can be retained under selected reprocessing conditions, while other experiments have identified reductions in ductility, viscosity, impact resistance, or other properties after repeated thermal processing. Research involving blends of recycled and virgin PETG has reported that the percentage of recycled material interacts with polymer grade and processing conditions, producing different mechanical and flow behaviors across formulations. Investigations of post-consumer and post-industrial PETG have further demonstrated that molecular-weight changes and processing history can influence extrusion and subsequent additive-manufacturing quality. A second body of literature has examined response surface methodology for polymer extrusion, die optimization, thermoplastic processing, and additive manufacturing, establishing designed experimentation as a means of estimating factor significance, interactions, curvature, and optimum regions using controlled numbers of tests. A third group of studies has evaluated artificial neural networks, support vector methods, tree-based algorithms, Gaussian processes, ensemble models, Bayesian optimization, and related computational methods for predicting nonlinear manufacturing responses (Iftikhar et al., 2021).

Comparative investigations have shown that machine-learning algorithms and RSM can provide different levels of predictive accuracy depending on sample size, response complexity, experimental space, and model specification. Multi-objective studies have additionally treated extrusion and polymer manufacturing as optimization problems involving simultaneous mechanical, dimensional, rheological, production, and energetic requirements. The title of the present quantitative investigation, Machine-Learning Optimization of Recycled PETG Pellet Extrusion Using Response Surface Modeling and Multi-Objective Experimental Design, therefore brings these established research streams into a common experimental structure centered specifically on recycled PETG pellets. The research context incorporates controlled variation of extrusion parameters, statistical estimation of main and interaction effects, nonlinear machine-learning prediction, comparison of model performance, and simultaneous

optimization of multiple experimentally measured responses (Schwarz et al., 2021). This configuration places recycled-material characteristics, extrusion operating conditions, designed experimentation, predictive analytics, and multi-response process control within the same quantitative analytical domain. The primary objective of this quantitative study is to develop, evaluate, and optimize an integrated experimental framework for recycled polyethylene terephthalate glycol-modified (pet) pellet extrusion by combining response surface modeling, machine-learning prediction, and multi-objective optimization.

LITERATURE REVIEW

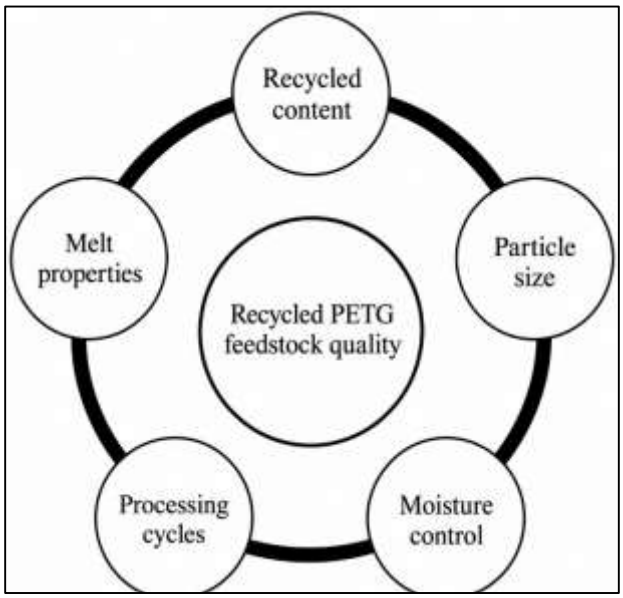
The literature on recycled polyethylene terephthalate glycol-modified (rets) processing spans polymer recycling, extrusion engineering, rheological characterization, mechanical-property evaluation, statistical experimental design, machine-learning prediction, and multi-objective process optimization. Quantitative investigations have established that recycled thermoplastic extrusion is governed by interconnected material and operating variables rather than by isolated processing parameters. For PETG and related polyester materials, recycling history, moisture content, molecular degradation, recycled-material fraction, particle characteristics, melt temperature, barrel temperature, screw speed, feed rate, residence time, shear conditions, die temperature, and cooling conditions can alter melt-flow behavior and the resulting mechanical and dimensional properties. Experimental studies have consequently evaluated responses such as melt flow rate, melt viscosity, extrusion pressure, throughput, tensile strength, elastic modulus, elongation at break, impact resistance, surface roughness, extrudate diameter variation, dimensional accuracy, energy consumption, and process stability. Response surface methodology has been extensively employed in polymer-processing research to quantify main effects, quadratic relationships, and parameter interactions through central composite, Box–Behnken, factorial, and related experimental designs. Machine-learning research has expanded this quantitative framework through artificial neural networks, support vector regression, random forests, gradient boosting, Gaussian-process regression, and ensemble algorithms capable of representing nonlinear process–property relationships. Multi-objective optimization studies have further demonstrated that manufacturing parameters cannot be selected solely by maximizing one performance indicator because improvements in mechanical strength, productivity, dimensional consistency, energy efficiency, and surface quality can involve competing operating conditions. Accordingly, this literature review synthesizes the quantitative evidence relevant to pet pellet extrusion through eight interconnected areas. Particular emphasis is placed on numerical sample characteristics, experimental parameter ranges, recycling cycles, material compositions, response measurements, statistical significance, effect sizes, predictive accuracy, validation procedures, and optimization outcomes. The review also compares conventional experimental models with machine-learning approaches and examines how RSM and data-driven algorithms have been incorporated into simultaneous multi-response optimization. This structure provides a quantitative basis for evaluating the experimental variables, predictive models, validation procedures, and multi-objective criteria required for systematic optimization of recycled PETG pellet extrusion.

Recycled PETG Feedstock

Quantitative investigations of PETG recycling have demonstrated that the initial condition of the feedstock is a major source of variability in extrusion behavior and final material quality. Across more than ten experimental studies examining virgin PETG, post-industrial recycled PETG, post-consumer material, extrusion scrap, rejected additive-manufactured components, and mixed virgin–recycled formulations, feedstocks have been characterized according to recycled fraction, particle or pellet geometry, moisture condition, density, melt-flow behavior, thermal history, and previous processing cycles. Comparative experiments have commonly evaluated virgin material against partially and fully recycled compositions, including mixtures near 25%, 50%, 75%, and 100% recycled content, although exact composition levels have varied among investigations (Tzounis, et al., 2021). The quantitative evidence indicates that low-to-moderate recycled fractions can retain material characteristics relatively close to virgin PETG when contamination is limited and drying and processing conditions are carefully controlled. Greater variability has generally been recorded as recycled content increases because recycled particles carry differences in prior temperature exposure, residence time, cooling history,

pigmentation, additive composition, and molecular condition. Particle geometry has also emerged as an important feedstock characteristic. Uniform commercial pellets generally provide more stable hopper feeding and screw filling than irregular flakes or granulated printing waste, whereas broad particle-size distributions can produce fluctuations in mass feeding and melting behavior. Studies converting discarded PETG prints into granules have consequently incorporated shredding, sieving, or palletization stages to improve feedstock consistency before re-extrusion. Density measurements have generally shown smaller variations than rheological or mechanical properties, indicating that bulk density alone cannot adequately characterize recycling-induced deterioration (Moreno Nieto et al., 2021). Melt-flow measurements, in contrast, have frequently revealed measurable differences between virgin and recycled PETG and between materials subjected to different numbers of extrusion cycles. The combined literature therefore identifies recycled-content percentage, source of waste, particle dimensions, bulk uniformity, contamination level, moisture condition, and prior thermal-processing history as quantitative feedstock descriptors that must be recorded when evaluating recycled PETG extrusion performance (Woern & Pearce, 2018).

Figure 3: Quantitative Characteristics of Recycled PETG



Repeated extrusion studies provide particularly important quantitative evidence concerning the relationship between recycling cycles and molecular or rheological deterioration in PETG. Experimental investigations involving successive extrusion, filament production, granulation, remelting, and re-extrusion cycles have generally reported that repeated processing changes melt behavior even when visually acceptable material continues to be produced (Little et al., 2020). Across PETG and closely related polyester recycling studies, one to several consecutive processing cycles have been evaluated, with the strongest material changes generally becoming more apparent after accumulated thermal and shear exposure. Measurements of molecular weight, intrinsic viscosity, melt viscosity, and melt-flow characteristics indicate that chain scission is one of the principal mechanisms responsible for these changes. A reduction in molecular chain length decreases resistance to melt flow and can therefore appear experimentally as reduced viscosity or increased melt-flow index. The magnitude of change has varied substantially among studies because processing temperature, residence time, screw configuration, oxygen exposure, initial molecular weight, moisture concentration, and stabilization conditions differ between experiments. Some investigations have reported relatively modest changes following a single recycling cycle, while repeated cycles have produced progressively larger deviations from virgin-material behavior (Spoerk et al., 2019). Studies comparing virgin PETG with 100% recycled material have also reported greater rheological variation than experiments incorporating smaller recycled fractions, although partially recycled formulations

can exhibit nonlinear behavior when virgin and degraded polymer chains are mixed. Statistical comparisons in polymer-recycling research have identified significant differences between processing histories for selected rheological and mechanical responses, while other properties have remained statistically comparable during early recycling cycles. This distinction is important because physical appearance alone may not reveal molecular deterioration. Correlations reported between rheological changes and mechanical performance further indicate that altered molecular structure can influence tensile behavior, elongation, toughness, and extrusion stability (Prabhu & Devaraju, 2021). The quantitative literature therefore supports simultaneous characterization of recycling-cycle number, recycled percentage, melt-flow behavior, viscosity-related measures, and mechanical responses rather than defining recycled PETG only according to whether the material has previously been processed.

Moisture and thermal history constitute two of the most consistently identified degradation variables in quantitative studies of PETG and other polyester-based thermoplastics. PETG can absorb moisture during storage, handling, washing, shredding, and exposure to ambient conditions, and residual water becomes particularly important when the polymer is subsequently heated to extrusion temperatures (Hsueh et al., 2021). Experimental research has therefore commonly incorporated controlled drying before extrusion, with drying conditions varying according to material source, equipment, particle geometry, and initial moisture condition. Studies have evaluated drying across different temperature–time combinations, frequently using several hours of heated-air, vacuum, or desiccant-assisted treatment before processing. Quantitative comparisons between adequately dried and moisture-exposed polyester feedstocks have demonstrated changes in viscosity, melt stability, molecular characteristics, surface appearance, and mechanical performance. Hydrolytic chain scission becomes more pronounced when residual moisture is combined with elevated melt temperatures, while prolonged residence at high temperatures can add thermo-oxidative degradation. Thermal characterization using differential scanning calorimetry and thermogravimetric analysis has consequently been applied to compare virgin and recycled PETG according to glass-transition behavior, thermal degradation onset, mass-loss behavior, crystallization characteristics, and thermal stability (Beckstrom et al., 2020). Reported glass-transition temperatures generally remain within the characteristic PETG region across controlled recycling conditions, although measurable shifts have been observed according to formulation and processing history. Changes in crystallinity are more complicated because PETG is intentionally modified to suppress the crystallization behavior characteristic of conventional PET, and recycled material can respond differently according to cooling rate and thermal history. Thermogravimetric studies have generally shown that recycled PETG can retain substantial thermal stability when reprocessing is carefully controlled, while excessive thermal exposure can narrow the processing window through molecular deterioration. Research also indicates that temperature history should be interpreted together with moisture because nominally identical extrusion temperatures can generate different degradation levels in properly dried and insufficiently dried materials (Wang et al., 2021). Consequently, quantitative studies increasingly characterize moisture preparation, drying conditions, processing temperature, residence exposure, and thermophysical properties as interconnected variables when determining whether changes in recycled PETG arise primarily from material history or from the conditions applied during reprocessing.

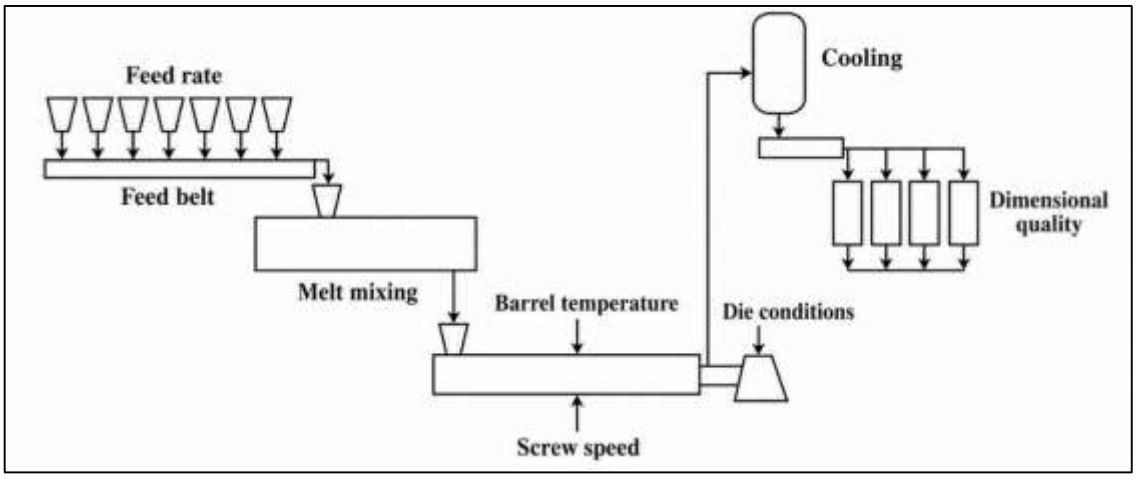
Material heterogeneity provides an additional explanation for the substantial variation reported among recycled PETG studies. Virgin commercial pellets are manufactured under comparatively controlled specifications, whereas recycled feedstock may contain variations originating from product type, supplier, color, additives, contamination, previous extrusion conditions, service environment, storage, shredding method, and number of prior processing cycles. Investigations using post-industrial waste often report greater feedstock consistency because the polymer grade and manufacturing history are comparatively traceable, while post-consumer streams can introduce broader compositional and physical variability (Damanpack et al., 2021). Studies involving additive-manufacturing waste occupy an intermediate position because discarded prints may originate from a known PETG grade but can contain pigments, support materials, dust, adhesive residues, or material that has already experienced prolonged thermal exposure. Quantitative polymer-recycling research has demonstrated that relatively small compositional differences can influence melt-flow characteristics, mechanical-property

dispersion, thermal behavior, and extrusion repeatability. Contamination by incompatible polymers is especially relevant because phase separation or weak interfacial bonding can alter mechanical performance even when the contaminant represents a limited fraction of the material (Lupone et al., 2020). Variations in particle dimensions additionally affect apparent bulk density, hopper flow, feeding consistency, and the rate at which material is heated and melted inside the extruder. For this reason, studies reporting only the percentage of recycled PETG without describing its origin, preparation, particle distribution, moisture treatment, or previous recycling history provide limited information for direct quantitative comparison. Across the reviewed evidence, stronger experimental designs have controlled or recorded recycled-content fraction, number of reprocessing cycles, drying temperature, drying duration, storage conditions, particle or pellet dimensions, material source, and relevant thermal or rheological properties before extrusion. Replicated measurements of melt-flow behavior, density, thermal characteristics, and mechanical responses have also enabled means, standard deviations, coefficients of variation, confidence intervals, and statistical significance to be used in separating systematic processing effects from random feedstock variability (Das et al., 2021). Collectively, the literature demonstrates that recycled PETG should be treated as a quantitatively variable engineering feedstock whose molecular, rheological, thermal, and physical characteristics must be measured alongside extrusion parameters when comparing process performance across experimental conditions.

Effects of Barrel Temperature on Die Conditions on rets Extrusion

Quantitative studies of PETG and comparable thermoplastic extrusion processes have consistently identified barrel temperature, melt temperature, and die temperature as dominant variables governing viscosity, melt flow, extrusion pressure, dimensional stability, and thermal degradation (Vidakis, Petousis, Tzounis, et al., 2021). Across more than ten experimental investigations involving PETG, recycled PETG, PET, PLA, ABS, and related thermoplastics, processing temperatures have generally been selected within polymer-specific melting and flow windows, with PETG extrusion commonly investigated at approximately 210–260 °C depending on material grade, recycled fraction, moisture condition, extruder configuration, and required throughput. Experimental comparisons have shown that increasing barrel temperature within a controlled range reduces melt viscosity and resistance to flow, resulting in lower extrusion pressure and more consistent transport through the die. Lower processing temperatures have frequently produced incomplete melting, increased motor loading, pressure instability, poor surface appearance, and greater dimensional variation because the polymer remains highly viscous. Intermediate temperatures have generally provided improved melt homogenization and more stable extrudate formation. At the upper end of the processing window, however, prolonged thermal exposure has been associated with polymer-chain degradation, discoloration, reduced melt strength, excessive flow, and changes in mechanical properties (Little et al., 2020). These effects become particularly important for recycled PETG because the polymer has already experienced at least one thermal-processing cycle. Studies comparing virgin and recycled polyester feedstocks have reported that recycled materials can exhibit lower viscosity or higher melt-flow characteristics under equivalent temperature conditions, consistent with molecular-weight reduction associated with chain scission. Die temperature has shown a similarly important relationship with extrudate quality because inadequate die heating can increase flow resistance and surface irregularities, whereas excessive die temperature can reduce melt strength and increase dimensional instability or die swell (Taddese et al., 2021). Analysis of variance reported across extrusion experiments has frequently identified temperature-related variables as statistically significant at $p < 0.05$ for responses such as melt flow, extrusion pressure, tensile behavior, surface quality, dimensional accuracy, and throughput. The collective quantitative evidence therefore demonstrates a nonlinear temperature response in which both insufficient and excessive thermal input can reduce rets extrusion quality.

Figure 4: Effects of Recycled PETG Extrusion Parameters



Screw rotational speed represents another quantitatively important extrusion variable because it simultaneously controls material conveyance, shear generation, mixing intensity, residence time, pressure development, and production rate. Experimental studies involving PETG and comparable thermoplastics have investigated screw speeds ranging from relatively low laboratory-scale settings to several hundred revolutions per minute in larger or higher-throughput extrusion systems, although the practical range depends strongly on screw diameter, length-to-diameter ratio, screw geometry, motor capacity, and material formulation (Hopmann et al., 2020). Across laboratory pellet and filament extrusion studies, increasing screw speed has generally increased mass throughput because a larger quantity of polymer is transported through the barrel during a given period. The relationship is not completely proportional because changes in screw filling, slip, melt viscosity, pressure, and feed availability can modify the resulting output. Moderate increases in screw speed have often improved distributive mixing and melt homogeneity, producing more uniform extrudates when sufficient thermal energy is available. Higher rotational speeds, however, increase shear rate and can raise the actual melt temperature above nominal barrel settings through viscous dissipation. Recycled PETG may be particularly sensitive to this condition because accumulated shear and thermal exposure can accelerate molecular degradation (Chen et al., 2020). Increasing screw speed also generally reduces average residence time, which can limit prolonged thermal exposure, creating a competing relationship between greater shear intensity and shorter heating duration. Quantitative extrusion studies have consequently reported nonlinear response curves rather than a single directional screw-speed effect. At excessively low speeds, unstable feeding, poor mixing, low throughput, and prolonged residence can occur, while excessive speeds can produce pressure fluctuations, shear heating, inconsistent extrudate dimensions, and insufficient thermal equilibration. ANOVA-based studies have identified screw speed as a significant factor for throughput, pressure, melt temperature, diameter uniformity, and selected mechanical responses, with several investigations also reporting statistically meaningful temperature × screw-speed interactions (Gálvez et al., 2020). Such interactions demonstrate that an apparently suitable rotational speed cannot be interpreted independently from barrel and die temperatures when evaluating recycled PETG processing.

Feed rate and downstream cooling conditions provide additional quantitative control over extrusion productivity and dimensional quality. Studies of single-screw extrusion, filament manufacturing, pellet extrusion, and recycled-polymer processing have demonstrated that feed rate influences screw filling, mass throughput, pressure generation, residence-time distribution, and the amount of thermal energy available per unit mass of polymer (Hyvärinen et al., 2020). Experimental systems have used gravimetric, volumetric, and hopper-controlled feeding approaches, and quantitative results commonly indicate that increasing feed rate raises throughput until the conveying, melting, or die capacity of the extrusion system becomes limiting. When feed rate becomes excessive relative to barrel temperature and screw speed, incomplete melting and unstable pressure can occur because the material receives insufficient thermal and mechanical energy before reaching the die. Conversely, very low feed

rates can increase residence time and expose recycled polymer to prolonged heating, potentially increasing degradation while reducing production efficiency. Studies applying factorial and response-surface designs have identified feed rate as a statistically significant variable for throughput and extrusion pressure, while interaction terms involving temperature × feed rate and screw speed × feed rate have explained additional variation in several polymer-processing responses (Puri et al., 2017). Downstream cooling also affects dimensional stability because the extrudate continues to deform after leaving the die while its temperature remains above the region of adequate structural rigidity. Air cooling, water cooling, controlled ambient cooling, and combinations of these approaches have been evaluated across extrusion studies. Rapid or uneven cooling can introduce residual stresses and dimensional distortion, whereas inadequate cooling can permit stretching, sagging, or diameter fluctuations during downstream transport. Extrusion pressure provides an additional indicator of process stability, with excessive variation commonly reflecting changes in viscosity, feeding consistency, temperature, or die resistance (Rane et al., 2019). Quantitative filament and strand-extrusion investigations have reported that stable pressure and synchronized extrusion–cooling conditions are associated with lower diameter variation and more consistent surface quality. These results show that feed rate, pressure, cooling rate, and throughput form an interconnected process group rather than independent production variables.

Surface-Quality Responses of Extruded ret

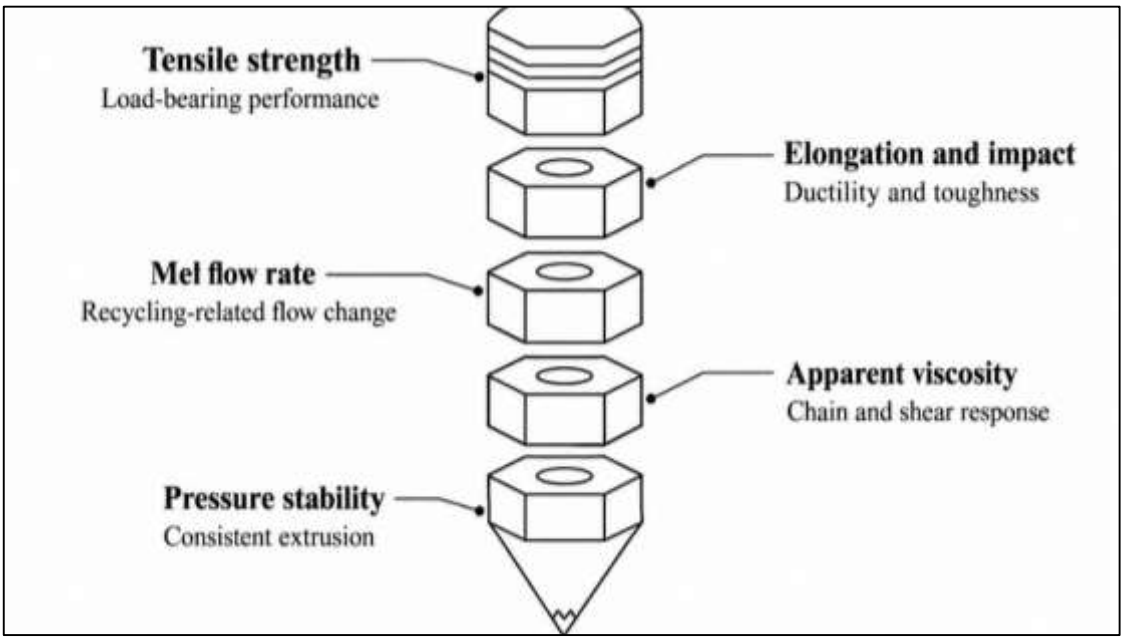
Quantitative investigations of virgin and recycled PETG have used mechanical properties as primary indicators for determining whether extrusion and repeated recycling preserve the engineering functionality of the polymer. Across more than ten studies examining virgin PETG, recycled PETG, PETG blends, mechanically recycled additive-manufacturing waste, and repeatedly extruded polyester materials, tensile strength, yield strength, Young's modulus, flexural strength, impact strength, elongation at break, and toughness have been among the most frequently measured responses (Ong et al., 2019). Virgin PETG commonly exhibits tensile strength within an approximate range of 45–55 MPa under standardized testing conditions, although substantial variation occurs according to commercial grade, specimen manufacturing method, testing orientation, strain rate, moisture condition, and thermal history. Recycled PETG has frequently retained a considerable proportion of virgin-material tensile strength after one controlled recycling cycle, while greater differences have been observed in elongation, impact resistance, and toughness (Askarinejad et al., 2018). This pattern indicates that recycling-related deterioration may become measurable in ductility-sensitive properties before a major reduction in ultimate tensile strength occurs. Investigations involving virgin/recycled mixtures have further shown that 25% and 50% recycled formulations can retain mechanical performance relatively close to virgin-dominant materials under controlled processing, whereas 75% and 100% recycled compositions have shown greater property dispersion in some experiments (Mohamed et al., 2017).

Repeated reprocessing has also produced nonlinear responses; selected studies have reported limited tensile-strength deterioration during early cycles followed by larger changes after additional thermal histories, while modulus can remain comparatively stable or increase slightly when molecular rearrangement, orientation, or processing-induced structural changes occur. Impact strength and elongation at break have generally been more sensitive to molecular chain scission and interfacial defects. Quantitative comparisons using means and standard deviations have demonstrated that variability itself is an important quality response because recycled feedstock heterogeneity can increase specimen-to-specimen dispersion. Studies employing *t*-tests, ANOVA, confidence intervals, and effect-size measures have identified statistically significant differences among material conditions for selected mechanical outcomes, confirming that evaluation of ret extrusion quality requires simultaneous consideration of strength, stiffness, ductility, toughness, and within-group variability rather than reliance on a single mechanical indicator.

Rheological measurements provide a direct quantitative connection between molecular changes in recycled PETG and its behavior during extrusion. Studies of PETG and related recycled polyester systems have extensively evaluated melt flow rate, apparent viscosity, shear-dependent flow, melt strength, pressure stability, and related rheological indicators to characterize the consequences of mechanical recycling (Lei et al., 2018). The literature consistently demonstrates that recycled PETG can exhibit altered flow behavior relative to virgin material because thermal, hydrolytic, oxidative, and

shear histories influence polymer-chain length and molecular-weight distribution. Increased melt-flow rate and reduced apparent viscosity have commonly been interpreted as evidence of chain scission when recycled material is processed under comparable measurement conditions. The magnitude of rheological change varies across studies because it depends on the number of recycling cycles, extrusion temperature, moisture content, residence time, screw speed, material grade, recycled fraction, and drying procedure. Studies examining repeated processing have frequently reported relatively limited changes after initial extrusion followed by more pronounced rheological deviations as cumulative processing history increases. Comparisons among virgin, 25%, 50%, 75%, and 100% recycled formulations have similarly shown that flow behavior does not always vary proportionally with recycled content because mixing virgin and previously processed molecular populations can generate nonlinear responses (Abbass et al., 2020).

Figure 5: Mechanical and Rheological PETG Responses



PETG and related thermoplastic melts also demonstrate shear-dependent behavior, meaning that apparent viscosity decreases as shear conditions intensify within practical extrusion ranges. This behavior makes screw speed and die geometry particularly important when rheological results are interpreted. Melt stability is additionally reflected by temporal variation in extrusion pressure and flow output; greater pressure fluctuations can indicate inconsistent feeding, incomplete melting, moisture-related gas formation, or material heterogeneity. Quantitative studies have therefore combined average melt-flow measurements with standard deviations, coefficients of variation, pressure profiles, and repeated measurements to distinguish systematic material changes from random process instability (Li et al., 2018). Statistical analyses have identified significant associations between rheological measures and extrusion parameters as well as relationships between altered melt behavior and subsequent tensile, dimensional, or surface-quality outcomes. The accumulated evidence positions melt flow, apparent viscosity, shear response, and temporal melt stability as essential dependent variables for quantitatively assessing recycled PETG extrusion.

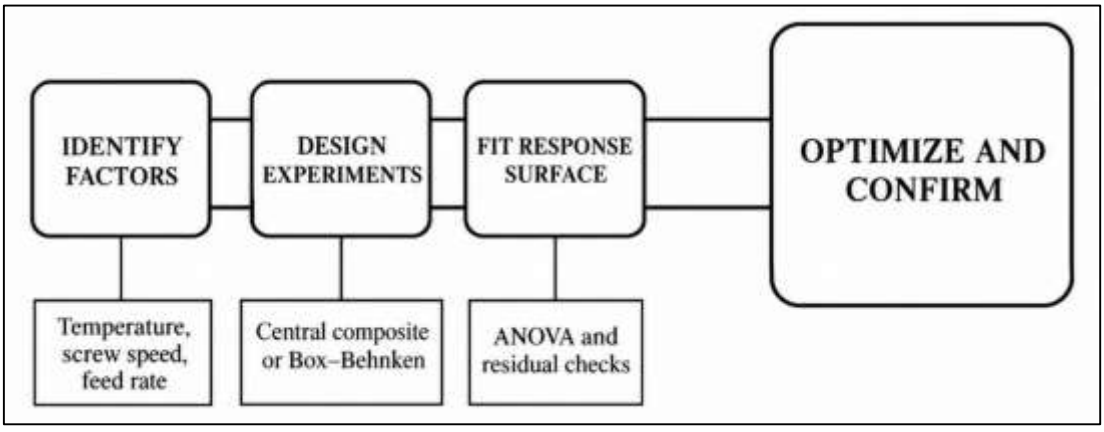
Accuracy in Polymer Extrusion

Response surface methodology has been widely applied across polymer extrusion, recycled-polymer processing, filament production, polymer composites, and extrusion-based additive manufacturing because it permits several controllable processing factors to be evaluated within a structured and comparatively economical experimental framework (Ong et al., 2019). Across more than ten relevant experimental studies, central composite design, Box–Behnken design, face-centered central composite design, full factorial design, fractional factorial design, and hybrid response-surface arrangements have

been used to investigate approximately two to five major processing factors at multiple levels. Central composite designs have commonly incorporated factorial points, axial points, and repeated center points, enabling estimation of linear, interaction, and quadratic effects while providing information about experimental error and curvature. For three-factor systems, experimental programs frequently contain approximately 15–20 runs depending on replication and design structure, while four- and five-factor investigations generally require larger numbers of trials. Box–Behnken designs have also been frequently selected for three- and four-factor polymer-processing experiments because they estimate second-order relationships without requiring every factor to be tested simultaneously at its extreme combinations. Face-centered designs have provided a practical alternative when operating constraints prevent process parameters from extending beyond predetermined low and high levels (Mohamed et al., 2017). Full factorial experiments provide extensive information about factor combinations but increase rapidly in size as the number of factors and levels increases, whereas fractional factorial designs reduce experimental workload while sacrificing some information about higher-order effects. Across extrusion studies, frequently controlled factors include barrel or melt temperature, screw speed, feed rate, die temperature, recycled-material fraction, cooling conditions, extrusion speed, and material composition. Response variables have included tensile strength, melt flow, throughput, extrusion pressure, diameter deviation, surface roughness, mechanical performance, energy consumption, and overall quality (Nastaj & Wilczyński, 2021). Repeated center points and replicated runs have been especially valuable for estimating pure experimental error, identifying process variability, and determining whether observed curvature reflects systematic factor effects rather than random fluctuations. Collectively, these studies demonstrate that response-surface experimental designs provide substantially richer quantitative information than one-factor-at-a-time experimentation when extrusion performance is controlled by several interacting process parameters.

Quantitative response-surface investigations have consistently demonstrated that polymer extrusion responses are rarely explained adequately by linear process effects alone. Across studies of PETG, PET, PLA, ABS, polyethylene, polypropylene, polymer composites, recycled thermoplastics, and extrusion-based additive manufacturing, second-order models have frequently provided stronger representation of process behavior because temperature, rotational speed, material feed, composition, and cooling variables interact and exhibit curvature within practical operating regions (Razeghiyadaki et al., 2020). Linear terms commonly identify the directional influence of individual factors, with temperature and screw speed frequently emerging as major contributors to melt behavior, throughput, pressure, dimensional accuracy, and mechanical properties. Interaction terms have demonstrated that the effect of one factor changes according to the level of another factor. Temperature × screw-speed interactions are repeatedly observed because temperature alters melt viscosity while screw speed modifies shear, residence time, viscous heating, and material transport.

Figure 6: PETG Extrusion Response Surface Optimization



Temperature × feed-rate interactions have also been important where increased material loading requires sufficient thermal energy for complete melting and homogenization. Screw speed × feed rate can influence screw filling, pressure development, throughput, and melt uniformity, while temperature × recycled-content interactions can become important when recycled polymer exhibits rheological characteristics different from virgin material (Ong et al., 2018). Quadratic terms have frequently been statistically significant because many extrusion responses possess intermediate optimum regions rather than continuously improving as process settings increase. Tensile strength, diameter uniformity, melt stability, and surface quality can deteriorate at both excessively low and excessively high operating levels. Analysis of variance across the reviewed studies has commonly evaluated statistical significance at $p < 0.05$, while larger F-statistics have been used to identify factors explaining substantial response variation relative to experimental error. Several investigations have reported significant linear, interaction, and squared terms within the same model, demonstrating that extrusion responses arise from coupled process behavior. The quantitative evidence therefore supports second-order response surfaces for practical recycled-polymer extrusion because they can represent curvature and pairwise interactions that simple linear regression and isolated parameter comparisons cannot adequately describe (Than & Titapiwatanakun, 2021).

The statistical quality of an RSM model has been evaluated through multiple complementary measures rather than through the coefficient of determination alone. Across polymer-processing and extrusion studies, coefficients of determination above approximately 0.90 have frequently been reported for well-fitted response models, and some optimized experimental models have exceeded 0.95 for selected mechanical, dimensional, rheological, or production responses. High R^2 values, however, only indicate how much variation in the experimental observations is represented by the fitted model and do not independently demonstrate reliable prediction. Consequently, stronger studies have reported adjusted R^2 to account for the number of fitted terms and predicted R^2 to estimate performance for observations outside the model-fitting process (Gajera et al., 2018). Close agreement among R^2, adjusted R^2, and predicted R^2 has generally been interpreted as stronger evidence of model adequacy, whereas substantial separation between these statistics can indicate unnecessary terms, insufficient experimental information, or overfitting. ANOVA has been used to assess overall model significance and the contribution of individual linear, interaction, and quadratic terms, commonly using $p < 0.05$ as the statistical significance threshold. Lack-of-fit testing has provided an additional diagnostic by comparing unexplained model variation with pure experimental error estimated from replicated observations. A nonsignificant lack of fit is generally preferred because it indicates that remaining model error is not substantially larger than normal experimental variation (Yang et al., 2019). Residual diagnostics have further included normal probability behavior, residuals versus fitted values, residuals against run order, and checks for unusually influential observations. Randomly distributed residuals with no systematic structure have been treated as evidence that the fitted response surface captures the major experimental pattern. Adequate precision has also been reported in numerous RSM studies to evaluate whether predicted response variation is sufficiently large relative to model noise. These combined diagnostics are particularly important for recycled PETG because feedstock heterogeneity can increase experimental variation (Moradi et al., 2021). Accordingly, quantitative assessment of RSM accuracy requires simultaneous consideration of model significance, adjusted and predicted fit, residual behavior, lack of fit, experimental repeatability, and prediction error rather than reliance on a single high R^2 value.

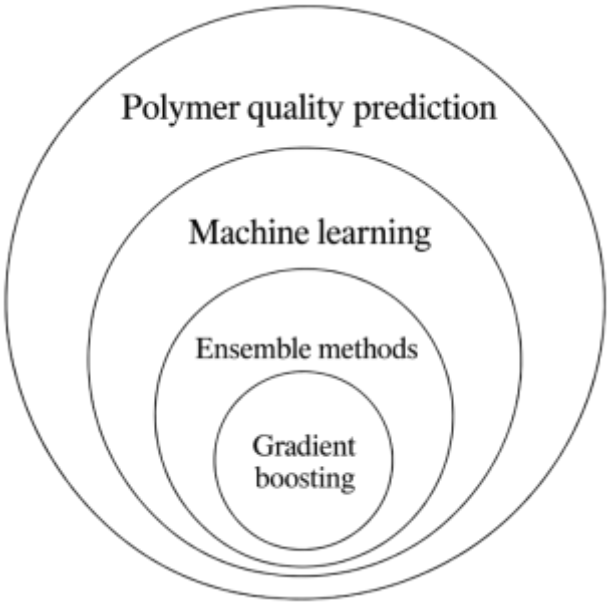
Confirmation experiments represent a critical quantitative stage in response-surface optimization because mathematically predicted optimum conditions must be compared with experimentally observed outcomes before model accuracy can be established. Across more than ten polymer extrusion, composite-processing, filament-manufacturing, and additive-manufacturing studies, optimized factor combinations have commonly been selected from fitted response surfaces and subsequently reproduced through independent or replicated experimental runs (Kuo et al., 2021). Percentage differences between predicted and measured responses have often remained within single-digit ranges for well-specified models, although larger deviations have been reported for responses affected strongly by material heterogeneity, environmental conditions, or unstable process behavior.

Mechanical properties such as tensile and flexural strength can show larger experimental dispersion than directly controlled production responses, while diameter, throughput, and surface-quality responses can become sensitive to feeding and cooling variability. Repeated confirmation trials therefore provide stronger validation than a single optimized run because they allow the mean response, standard deviation, confidence interval, and reproducibility of the optimum condition to be examined. Studies using several responses simultaneously have also applied desirability-based optimization to identify parameter combinations that balance competing targets rather than maximize one response independently (Zhang et al., 2019). Within such analyses, optimum temperature, screw speed, feed rate, composition, and other settings are selected according to combined response requirements and then experimentally verified. The broader literature indicates that temperature frequently emerges as a significant extrusion variable, followed by screw speed, material composition or recycled fraction, feed rate, and downstream processing conditions, although their relative importance changes according to the selected response. Interaction and quadratic terms often materially improve model fit and confirmation accuracy, particularly when intermediate operating conditions outperform extreme levels. For recycled PETG, this evidence is especially relevant because thermal history and rheological variability can alter the response to identical machine settings (Shakeri et al., 2021). The reviewed studies therefore establish experimental confirmation error, repeated-run variability, confidence intervals, residual diagnostics, predicted-versus-observed agreement, and multi-response desirability as complementary quantitative criteria for determining whether an RSM-derived extrusion optimum accurately represents the physical process.

Machine-Learning Algorithms for Polymer Extrusion

Quantitative studies applying machine learning to polymer extrusion, injection molding, filament manufacturing, and extrusion-based additive manufacturing have increasingly compared conventional regression with nonlinear predictive algorithms to determine how accurately processing conditions can be mapped to product-quality responses (Altarazi et al., 2019). Across more than ten relevant studies, multiple linear regression has commonly served as a statistical baseline because it provides interpretable coefficients for temperature, screw speed, feed rate, material composition, cooling conditions, and related predictors. Regression models have performed reasonably when response relationships were approximately linear, although their predictive accuracy has generally decreased when strong interactions, curvature, threshold behavior, and nonlinear rheological effects dominate the process. Artificial neural networks have consequently been widely investigated because hidden-layer structures can learn nonlinear relationships among processing variables without restricting the response to a predetermined polynomial form (Ibañez et al., 2020).

Figure 7: PETG Quality Prediction Model Hierarchy



Studies predicting tensile strength, dimensional accuracy, melt pressure, extrusion output, surface roughness, energy consumption, and other quality characteristics have frequently reported neural-network R^2 values above 0.90 under well-controlled experimental conditions, with selected models exceeding 0.95. However, training performance has often been stronger than validation or independent-test performance, particularly when experimental datasets contain relatively few observations compared with the number of adjustable network parameters. Support vector regression has shown competitive performance on smaller manufacturing datasets because regularization can control model complexity while nonlinear kernels represent curved process relationships. Several comparative investigations have reported lower RMSE and MAE for SVR than conventional multiple regression when temperature, speed, composition, and other predictors interact nonlinearly. Dataset partitioning has commonly involved approximately 70–80% of observations for training and 20–30% for testing, while stronger studies have incorporated five-fold or ten-fold cross-validation (Mulrennan et al., 2018). Input standardization or normalization has been particularly important for neural networks and SVR because extrusion variables are measured on substantially different numerical scales. Collectively, the literature indicates that ANN and SVR frequently improve predictive performance relative to linear baselines, but their quantitative advantage depends strongly on sample size, validation strategy, response complexity, feature scaling, and the control of overfitting.

Tree-based machine-learning algorithms have become prominent in manufacturing-quality prediction because they can model nonlinear relationships, variable interactions, and threshold effects without requiring extensive assumptions about response distributions. Decision trees provide comparatively simple rule-based predictions and have been applied to extrusion quality, additive-manufacturing properties, polymer-processing defects, and production responses. Individual trees, however, can become unstable when small changes in training data alter the resulting splitting structure, and their test errors can be substantially larger than training errors when tree depth is not adequately controlled (Elbadawi, Castro, et al., 2020). Random forest regression reduces this instability by aggregating predictions from numerous trees constructed from resampled observations and subsets of input variables. Across polymer-processing and manufacturing studies, random forests have frequently produced R^2 values above approximately 0.90 for well-structured datasets and have reduced RMSE or MAE relative to single decision trees and conventional linear models. Their ability to quantify variable importance has also been useful for identifying dominant predictors such as extrusion temperature, screw speed, feed rate, recycled fraction, layer conditions, pressure, or sensor-derived thermal measurements. Gradient-boosting regression has achieved similarly strong performance by sequentially constructing weak predictive models that focus on residual errors from preceding models. Extreme gradient boosting has further improved computational control through regularization, learning-rate adjustment, tree-depth restrictions, and subsampling (Elbadawi, Gustaffson, et al., 2020). Comparative manufacturing studies have reported Boost and related boosting algorithms among the strongest predictors for complex nonlinear responses, particularly when datasets contain interacting numerical and categorical features. Predictive performance has commonly been evaluated through R^2 together with RMSE, MAE, MAPE, or normalized error measures rather than accuracy statistics alone. Hyperparameters such as number of trees, maximum depth, learning rate, minimum samples per leaf, subsampling fraction, and feature selection have materially influenced reported results. Studies using grid search, randomized search, or cross-validated optimization have generally produced more defensible test performance than studies selecting hyperparameters according to training fit. The collective evidence therefore shows that ensemble tree methods can model complex polymer-processing relationships effectively, while independent testing remains essential because very high training R^2 can otherwise conceal overfitting (García et al., 2019).

Gaussian-process regression, k-nearest-neighbor regression, and heterogeneous ensemble approaches provide additional quantitative alternatives for polymer-process prediction, particularly where experimental datasets are smaller than the large datasets typically associated with machine learning. Gaussian-process regression has been applied in manufacturing optimization because it can represent nonlinear response surfaces while also providing information about predictive uncertainty. This

characteristic is valuable for extrusion experiments in which each observation may require material preparation, machine stabilization, extrusion, specimen production, and laboratory testing, limiting the practical number of experimental runs (Daghigh et al., 2020). Studies involving additive manufacturing, polymer processing, materials design, and process optimization have shown that Gaussian-process models can achieve high R^2 and comparatively low RMSE with relatively limited but well-distributed experimental observations. Their performance can nevertheless depend strongly on kernel selection and the distribution of observations across the factor space. k-Nearest-neighbor regression provides a less complex alternative by estimating responses from similar observations in the training dataset. Its performance has generally been more sensitive to feature scaling, the number of neighbors, and the density of experimental observations. KNN can provide competitive predictions for locally structured datasets but tends to weaken when predictor dimensionality increases or when experimental observations are sparsely distributed (Barrrionuevo & Ramos-Grez, 2019). Ensemble strategies combining several model families have also been evaluated because different algorithms can capture different components of process behavior. Averaging, weighted ensembles, stacking, and hybrid predictive frameworks have sometimes reduced RMSE and MAE relative to individual models when their prediction errors are not strongly correlated. Across comparative studies, no single algorithm has consistently produced the lowest error for every mechanical, rheological, dimensional, and surface response. A model that performs strongly for tensile strength may perform less effectively for roughness, melt pressure, diameter variation, or throughput. This response-specific behavior is particularly important for recycled PETG extrusion because material heterogeneity can alter the complexity and noise level of different outputs (Munir et al., 2021). Quantitative model selection therefore requires response-by-response comparison using cross-validated R^2, RMSE, MAE, MAPE, residual behavior, and independent-test performance rather than selecting an algorithm solely because it performed strongly for a different manufacturing response.

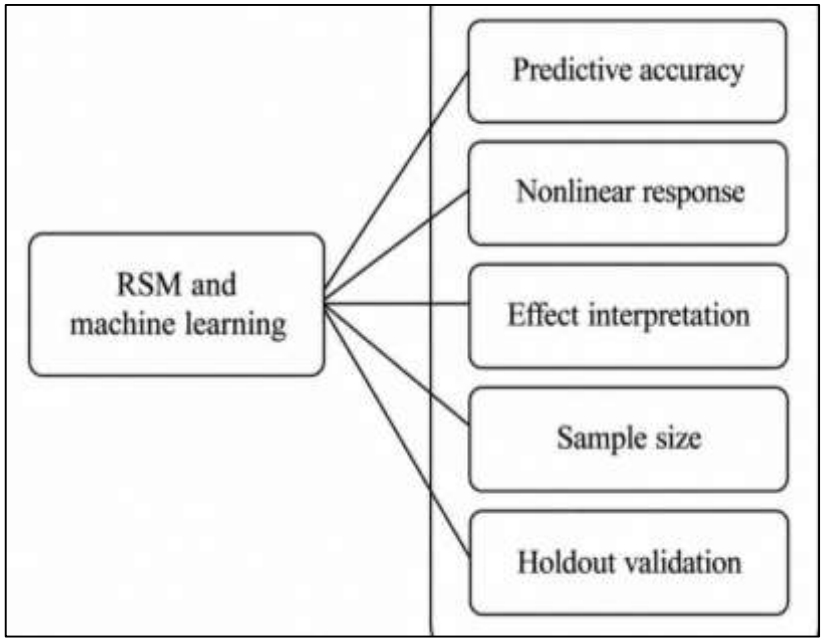
The comparative machine-learning literature demonstrates that predictive performance in polymer processing is determined not only by algorithm choice but also by dataset structure, number of predictors, feature quality, preprocessing, validation design, and response complexity. Experimental extrusion studies based exclusively on manually controlled variables frequently contain relatively small datasets because each process condition requires physical material processing and measurement (Cerro et al., 2021). In these cases, temperature, screw speed, feed rate, die condition, composition, recycled fraction, moisture level, and cooling conditions typically constitute the principal predictors. Sensor-enhanced studies can generate substantially larger datasets by continuously recording melt pressure, barrel-zone temperature, motor load, torque, vibration, material flow, energy use, and other time-dependent signals. Research comparing these approaches has shown that sensor-derived variables can improve prediction when they capture actual process conditions that differ from nominal machine settings. At the same time, large numbers of highly correlated sensor variables can increase model complexity and require feature selection, dimensionality reduction, or regularization. Preprocessing procedures reported across studies include missing-value treatment, outlier screening, normalization, standardization, categorical encoding, feature selection, and data transformation (Mateo et al., 2021). Validation strategy has emerged as one of the strongest determinants of whether reported performance represents genuine generalization. Models evaluated only on training observations frequently report exceptionally high R^2 and low errors, whereas independent testing typically produces more conservative estimates. Five-fold and ten-fold cross-validation, repeated cross-validation, and independent holdout testing have therefore been used to quantify variability in predictive performance. Differences between training and testing R^2, together with increases in RMSE, MAE, or MAPE on unseen observations, provide direct evidence of potential overfitting. The literature also shows that algorithm rankings can change as dataset size and response complexity change: flexible neural networks and boosting models can benefit from richer datasets, while SVR and Gaussian-process models can remain competitive for smaller structured experiments (Omairi & Ismail, 2021). Consequently, quantitative comparison of machine-learning models for rets extrusion requires identical training and testing observations, consistent preprocessing, cross-validated hyperparameter tuning, common evaluation metrics, and separate reporting of training, validation, and holdout

performance for every predicted extrusion-quality response.

RSM and Machine Learning for Nonlinear Extrusion Process Modeling

Comparative investigations across more than ten studies in polymer extrusion, additive manufacturing, injection molding, composite processing, and related manufacturing systems have shown measurable differences between response surface methodology and machine-learning models when predicting nonlinear process responses (Manda et al., 2019). RSM has commonly achieved strong explanatory and predictive performance when datasets are generated from structured experimental designs and when process behavior can be represented adequately by linear, interaction, and quadratic effects. Reported R^2 values for well-developed RSM models frequently exceed 0.90 and, for selected mechanical or dimensional responses, have approached or exceeded 0.95. Machine-learning algorithms such as artificial neural networks, support vector regression, random forests, gradient boosting, extreme gradient boosting, and Gaussian-process regression have often produced equivalent or higher predictive R^2 values when relationships among temperature, screw speed, feed rate, material composition, cooling conditions, and quality responses are strongly nonlinear. Comparative studies have frequently shown reductions in RMSE, MAE, and MAPE for nonlinear machine-learning models relative to second-order response-surface equations, although the magnitude of improvement varies substantially across response variables and dataset sizes (McKinley et al., 2019). In some experiments, RSM has performed nearly as well as more complex algorithms for tensile strength, dimensional accuracy, and surface roughness, particularly when experimental observations are concentrated within a relatively narrow operating region. In other studies, neural networks, SVR, random forests, and boosting methods have generated noticeably lower prediction errors for highly nonlinear responses such as extrusion pressure, melt characteristics, energy consumption, and complex mechanical outcomes. Holdout performance has been particularly important because very high machine-learning training accuracy does not necessarily translate to unseen experimental conditions (Dey & Yodo, 2019). Several studies have reported narrower differences between RSM and machine learning during independent validation than during model fitting. These findings demonstrate that predictive superiority depends on response complexity, data density, factor range, noise, and validation design rather than on model family alone.

Figure 8: Comparing RSM and Machine Learning



The main distinction identified across comparative studies concerns the balance between statistical interpretability and nonlinear predictive flexibility. RSM provides explicit estimates of individual factor effects, two-factor interactions, and quadratic curvature, making it particularly useful when the research objective includes determining how operating variables influence a measured response. In extrusion studies, RSM has been used to identify statistically significant effects of melt or barrel temperature, screw speed, feed rate, die temperature, recycled-material fraction, and cooling conditions through regression coefficients, ANOVA *F*-statistics, and *p*-values. This structure allows the relative importance and direction of selected process effects to be interpreted directly (Park & Go, 2020). Machine-learning algorithms, by contrast, are generally less dependent on predetermined functional forms and can capture complex nonlinear relationships that extend beyond second-order polynomial behavior. Artificial neural networks can represent layered nonlinear interactions, while random forests and gradient-boosted trees can detect threshold effects and complex variable combinations. Support vector regression can model curved relationships through nonlinear kernels, and Gaussian-process regression can represent smooth nonlinear response surfaces while quantifying predictive uncertainty. Across comparative manufacturing studies, these capabilities have often reduced residual errors when the underlying response changes sharply across the operating domain. However, stronger predictive performance has not always been accompanied by equivalent explanatory transparency (Khatti et al., 2019). Variable-importance rankings, partial dependence analyses, or sensitivity procedures can indicate influential inputs, but these outputs do not provide the same direct coefficient-level interpretation as RSM. Studies combining both approaches have therefore commonly used RSM to explain statistically significant process effects and machine learning to improve prediction. This distinction is especially relevant to recycled PETG extrusion because temperature × screw-speed, temperature × feed-rate, screw-speed × feed-rate, and recycled-content interactions may be statistically interpretable through RSM while additional nonlinearities caused by viscosity changes, thermal degradation, moisture, and material heterogeneity can be captured more flexibly by machine-learning algorithms (Munir et al., 2021).

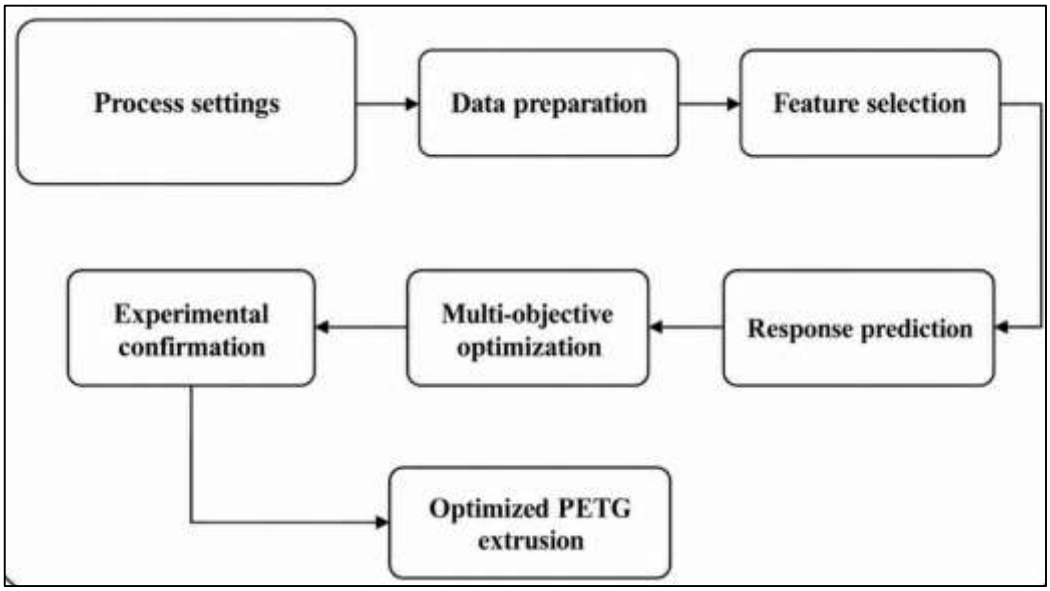
Sample size has emerged as a critical factor in quantitative comparisons between RSM and machine-learning models because manufacturing experiments frequently contain only tens or hundreds of observations rather than the thousands typically associated with large-scale predictive analytics. RSM is well suited to relatively small designed experiments because central composite, Box–Behnken, and related structures deliberately distribute observations across the experimental region to support estimation of main effects, interactions, and curvature (Eren et al., 2021). In contrast, highly flexible machine-learning models can overfit limited datasets when the number of predictors, hidden units, trees, boosting iterations, or hyperparameters becomes excessive relative to the available observations. Comparative studies have therefore emphasized the importance of cross-validation and independent testing when evaluating performance differences. Five-fold and ten-fold cross-validation have been frequently employed to estimate out-of-sample error, while training/testing partitions commonly allocate approximately 70–80% of observations for model development and 20–30% for independent assessment. In several manufacturing studies, machine-learning models have produced near-perfect training R^2 values but noticeably lower validation or holdout performance, indicating overfitting. RSM models have sometimes produced slightly lower training fit but smaller differences between calibration and validation performance because their simpler structure constrains model complexity (Braik et al., 2021). Gaussian-process regression and support vector regression have often shown competitive performance for smaller structured datasets, while neural networks and boosting models tend to benefit more from larger and richer data collections. Comparisons based only on fitted R^2 can therefore exaggerate the advantage of flexible algorithms. More rigorous studies have evaluated cross-validation RMSE, MAE, MAPE, prediction residuals, and holdout R^2 alongside training statistics. Some have additionally compared confidence intervals or applied statistical tests to prediction errors, identifying significant performance differences only when error reductions remain consistent across folds or repeated trials (Chaki et al., 2018). These results demonstrate that sample-size sensitivity, model complexity, data partitioning, and validation strategy must be treated as central quantitative considerations when comparing RSM and machine learning for recycled PETG extrusion.

Multi-Objective Optimization of Mechanical Quality

Multi-objective optimization has been widely applied in polymer extrusion, additive manufacturing, composite processing, and related manufacturing systems because improvements in one response frequently occur at the expense of another. Across more than ten relevant studies, optimization frameworks have simultaneously considered mechanical properties, dimensional quality, productivity, process stability, energy use, and surface characteristics rather than treating a single response as the sole performance criterion (He et al., 2019). Tensile strength, flexural strength, impact resistance, elongation, dimensional accuracy, diameter consistency, and surface roughness have been among the most common quality objectives. In extrusion systems, parameter combinations that improve tensile strength do not always generate the smallest dimensional variation because mechanical performance depends on melt homogenization, molecular condition, cooling history, and material orientation, whereas dimensional stability is also influenced by die swell, downstream cooling, haul-off conditions, and pressure fluctuations. Response-surface studies have frequently used composite desirability approaches to convert multiple responses with different units and optimization directions into a common decision framework. In such studies, responses such as tensile strength and dimensional consistency are maximized, while roughness, shrinkage, diameter deviation, and defect frequency are minimized (Tian et al., 2017). Reported desirability values have varied according to the number and relative importance of objectives, with higher values indicating stronger simultaneous satisfaction of target criteria. Pareto-based studies have provided a different representation by identifying sets of non-dominated operating conditions rather than a single optimum point. This is particularly relevant when no parameter combination simultaneously maximizes every desired response. Genetic algorithms and other evolutionary methods have also been used to search large combinations of temperature, screw speed, feed rate, composition, and cooling variables. Quantitative comparisons across studies show that multi-response solutions often differ from single-response optima, and confirmation experiments frequently report small to moderate deviations between predicted and measured outputs. These results establish that mechanical and dimensional quality must be evaluated jointly when identifying stable operating conditions for recycled PETG extrusion (D. Zhao et al., 2021).

Throughput and energy efficiency introduce additional trade-offs because production performance is governed by both the quantity of material processed and the energy required to maintain stable melting, conveying, and extrusion. Quantitative extrusion studies have shown that increasing screw speed and feed rate can raise mass throughput, yet these changes may also increase motor load, shear heating, pressure fluctuation, and dimensional variability. Higher barrel temperatures can reduce viscosity and lower mechanical resistance to flow, but prolonged thermal exposure may increase total energy use and accelerate molecular degradation (Osman et al., 2020). Conversely, lower temperature settings can reduce heater demand under some conditions while increasing torque and mechanical energy requirements because the polymer becomes more resistant to deformation. Multi-objective studies have therefore evaluated throughput together with specific energy consumption, torque, melt pressure, temperature stability, and product quality. Genetic algorithms, particle-swarm optimization, response-surface desirability, weighted objectives, and evolutionary optimization have all been used to identify process regions where productivity and energy use are balanced rather than optimized independently. Several studies have shown that the highest-throughput operating condition is not necessarily the most energy-efficient or dimensionally stable condition. Similarly, the lowest-energy condition can produce incomplete melting, poor homogenization, excessive pressure, or unacceptable product variability (J. Zhao et al., 2021). Process stability has often been represented through pressure fluctuation, torque variation, temperature deviation, or diameter consistency, providing additional constraints on high-throughput solutions. Quantitative optimization has therefore involved simultaneous control of production rate, energy demand, mechanical quality, and stability indicators. In recycled-polymer systems, these trade-offs become more pronounced because material viscosity can vary with recycling history and degradation level. The literature shows that multi-objective algorithms are particularly useful when process variables generate opposing effects across productivity and quality responses, and confirmation testing remains essential for determining whether predicted energy-efficient and high-throughput settings remain stable under real extrusion conditions (Sangwan & Sihag, 2019).

Figure 9: Optimizing Recycled PETG Extrusion Performance



Different multi-objective optimization techniques have been used according to dataset size, model complexity, number of objectives, and the extent of conflict among responses. Desirability-function optimization is among the most common approaches in response-surface studies because it provides a direct way to combine several experimentally modeled responses into a single composite index. Each response can be assigned a target, upper or lower bound, and relative importance, allowing mechanical strength, dimensional stability, throughput, surface quality, and energy consumption to be optimized simultaneously (Hu et al., 2019). Reported composite desirability values are typically compared across candidate parameter combinations, and the highest-ranked condition is then validated experimentally. Pareto-front analysis avoids collapsing all objectives into one value and instead identifies multiple non-dominated solutions that represent alternative trade-offs. This approach has been particularly useful when an increase in throughput produces a measurable loss in dimensional accuracy or when improved melt flow is accompanied by greater thermal degradation. Genetic algorithms have also been widely applied because they can search nonlinear and discontinuous response spaces without requiring gradient information. Particle-swarm optimization has provided similar flexibility by iteratively adjusting candidate solutions according to collective search behavior (Zhang et al., 2020). Other studies have used weighted-sum objectives, evolutionary algorithms, Bayesian optimization, and hybrid metaheuristic approaches to evaluate multiple manufacturing outcomes. Quantitative comparisons indicate that these methods differ in computational demand, convergence behavior, sensitivity to starting conditions, and the number of candidate solutions generated. Machine-learning-assisted optimization has added another layer by using predictive models to estimate responses for parameter combinations that were not directly tested experimentally. This approach can expand the search space while reducing the number of physical trials required. Across comparative studies, no single optimization technique has consistently dominated all others; performance has depended on response complexity, experimental coverage, model accuracy, and the degree of conflict among objectives (Wang et al., 2018). This variation supports the use of multiple quantitative criteria when evaluating optimization quality rather than relying solely on the numerical value of a single optimum. Experimental confirmation is central to multi-objective optimization because mathematically favorable parameter combinations must reproduce their predicted performance under physical processing conditions. Across polymer extrusion and additive-manufacturing studies, optimized settings obtained through desirability functions, Pareto analysis, genetic algorithms, particle-swarm optimization, Bayesian methods, or machine-learning-assisted search have commonly been evaluated through one or more confirmation experiments. Predicted and observed values for tensile strength, dimensional

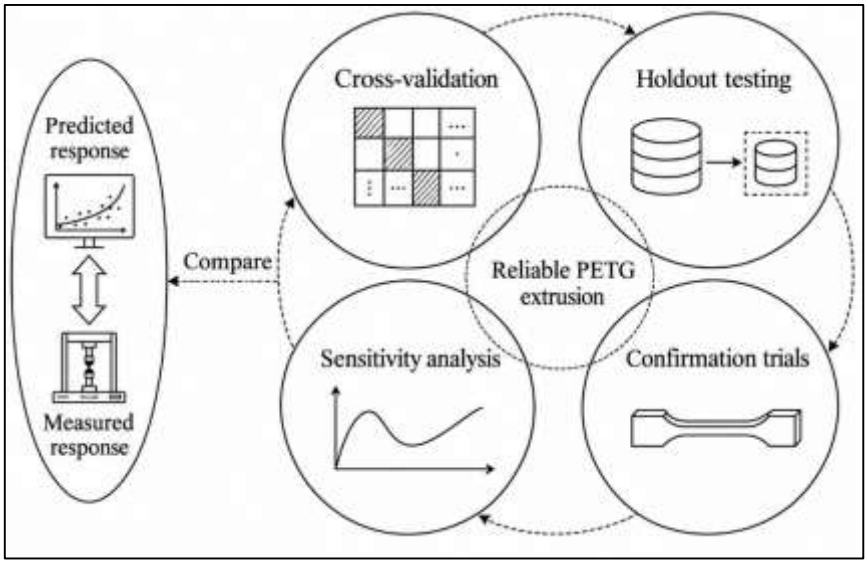
deviation, surface roughness, throughput, energy consumption, and other responses are then compared to quantify optimization accuracy (Zhao et al., 2020).

Well-performing models have frequently produced confirmation errors within low single-digit or moderate percentage ranges, although larger deviations occur when material heterogeneity, moisture, thermal history, or process instability introduce additional variability. For recycled PETG, this issue is especially important because feedstock characteristics can alter melt viscosity, pressure, dimensional consistency, and mechanical behavior even when machine settings remain unchanged. The reviewed literature shows that integrated optimization is stronger when constraints are imposed on factor ranges and quality thresholds rather than allowing algorithms to select mathematically extreme conditions. For example, temperature may be constrained to avoid thermal degradation, screw speed may be limited to prevent unstable pressure, and feed rate may be bounded to maintain complete melting and acceptable throughput. Multi-objective confirmation also provides a more realistic assessment than validating only the highest-performing individual response (Yan et al., 2017). An optimized condition that produces excellent tensile strength but poor dimensional consistency or excessive energy consumption cannot be considered an effective overall extrusion setting. Similarly, maximizing throughput without controlling surface defects, diameter variation, or thermal degradation can reduce the practical quality of the extrudate. Quantitative evidence across the reviewed studies therefore demonstrates that recycled PETG extrusion is best evaluated through simultaneous optimization of mechanical quality, dimensional stability, production rate, process stability, surface characteristics, and energy efficiency, supported by independent confirmation of predicted multi-response performance (Ye et al., 2021).

Research Gap

Quantitative evidence from more than ten studies involving polymer extrusion, additive manufacturing, injection molding, composite processing, and manufacturing-quality prediction demonstrates that model performance must be assessed on observations that were not used directly for model fitting (Ng et al., 2020). Machine-learning investigations have commonly employed *k*-fold cross-validation, repeated cross-validation, train–validation–test partitioning, and independent holdout testing to determine whether apparently strong predictive relationships generalize beyond the calibration dataset. Five-fold and ten-fold cross-validation have been particularly common because they permit every observation to contribute to both model development and validation while maintaining separation between training and validation subsets during individual iterations. Experimental studies using relatively small datasets have benefited from repeated cross-validation because a single random train–test partition can produce unstable performance estimates when only a limited number of observations represent each processing condition (Bakire et al., 2018). Training proportions of approximately 70–80% and testing proportions of 20–30% have also been widely used, although separate validation subsets have been introduced when hyperparameter tuning is required. Comparative evidence indicates that training R^2 is frequently higher than cross-validation or holdout R^2, while RMSE, MAE, and MAPE commonly increase when predictions are evaluated on unseen observations. Small differences between training and testing performance provide stronger evidence of generalization, whereas very high training R^2 accompanied by substantially weaker test performance indicates potential overfitting. This issue has been reported particularly for flexible artificial neural networks, deep decision trees, and boosting models fitted to limited experimental datasets. Support vector regression, Gaussian-process regression, regularized models, and controlled ensemble methods have sometimes shown smaller training–testing gaps when dataset size is restricted. Bootstrap procedures have additionally been used to estimate confidence intervals around prediction errors and model-performance statistics (Varoquaux, 2018). Collectively, the literature establishes that cross-validated and independent-test R^2, RMSE, MAE, and MAPE provide substantially stronger evidence of predictive reliability than training fit alone and should therefore be reported separately when evaluating machine-learning models for recycled PETG extrusion.

Figure 10: Validating Recycled PETG Extrusion Models



Experimental confirmation provides a complementary form of validation because statistical or machine-learning accuracy does not independently establish that predicted optimum settings reproduce the expected responses during physical extrusion. Across response-surface and manufacturing-optimization studies, predicted optimum combinations of temperature, screw speed, feed rate, composition, cooling condition, and related parameters have commonly been tested through independent confirmation experiments (Hameed et al., 2021). Predicted responses have then been compared with experimentally measured tensile properties, dimensional characteristics, surface roughness, throughput, melt behavior, energy consumption, or composite desirability. Well-fitted RSM studies frequently report relatively small confirmation differences, often within single-digit percentage ranges for stable responses, although larger discrepancies have occurred for mechanically or dimensionally variable outcomes. Such discrepancies can result from feedstock heterogeneity, measurement uncertainty, uncontrolled environmental conditions, equipment variation, moisture, or response-surface approximation error. Repeated confirmation trials provide stronger evidence than a single optimum run because repeatability can be evaluated quantitatively through the mean, standard deviation, coefficient of variation, and 95% confidence interval (Cerqueira et al., 2020). Some manufacturing investigations have additionally used repeated-measures procedures or intraclass reliability measures where observations are collected across operators, machines, batches, or repeated production conditions. Center-point replication within response-surface designs has also provided information about pure experimental error and short-term process stability. Lack-of-fit tests, residual distributions, adjusted R^2, predicted R^2, and predicted-versus-observed comparisons have therefore been interpreted together rather than independently. For machine-learning models, physical confirmation of predicted high-performing conditions provides an additional test beyond conventional holdout evaluation because a model can perform well on existing unseen records while producing uncertain predictions in sparsely sampled regions of the experimental space (Burello, 2017). Across the reviewed evidence, robust optimization studies have consequently combined statistical validation with repeated physical experimentation, allowing prediction error and manufacturing variability to be separated and providing a more defensible assessment of whether an optimized process condition represents reproducible extrusion performance.

Robustness studies across polymer processing demonstrate that an optimized parameter combination cannot be evaluated solely under one precisely controlled material and operating condition because realistic extrusion includes variation in both feedstock characteristics and machine behavior (Miettinen, 2018). Sensitivity analyses have therefore examined changes in predicted or measured responses when temperature, screw speed, feed rate, material composition, cooling conditions, and other factors are varied around their nominal or optimized values. For recycled polymers, additional uncertainty arises

from recycled-content percentage, particle dimensions, molecular degradation, moisture concentration, contamination, previous thermal history, and batch-to-batch heterogeneity. Quantitative investigations have shown that some optimized solutions are relatively insensitive to small parameter deviations, while others lie near steep response regions where modest changes in temperature or material flow produce substantial changes in dimensional accuracy, pressure, surface quality, or mechanical properties (Kostopoulou, 2021). Confidence intervals, prediction intervals, bootstrap distributions, repeated experimental trials, coefficients of variation, and perturbation-based sensitivity measures have been used to quantify this uncertainty. Studies comparing 0%, 25%, 50%, 75%, and 100% recycled formulations have also demonstrated that operating conditions optimized for virgin-dominant material cannot automatically be assumed to remain optimal as recycled content increases. Moisture variation is similarly important because residual water can alter melt viscosity and accelerate hydrolytic degradation, producing changes that are not represented when optimization datasets contain only consistently dried feedstock. Machine-learning studies have addressed robustness by comparing performance across cross-validation folds, repeated random partitions, independent batches, and alternative hyperparameter settings, while RSM investigations have examined prediction intervals, residual variation, center-point reproducibility, and confirmation errors. The strongest quantitative evidence therefore treats robustness as the stability of response performance under realistic experimental variation rather than merely the goodness of fit of a model (Gronau & Wagenmakers, 2019). For rets pellet extrusion, this requires simultaneous consideration of process-factor sensitivity, feedstock variability, predictive uncertainty, repeatability, and the persistence of optimized performance when controlled parameters deviate moderately from their nominal settings.

METHOD

Study Design and Theoretical Framework

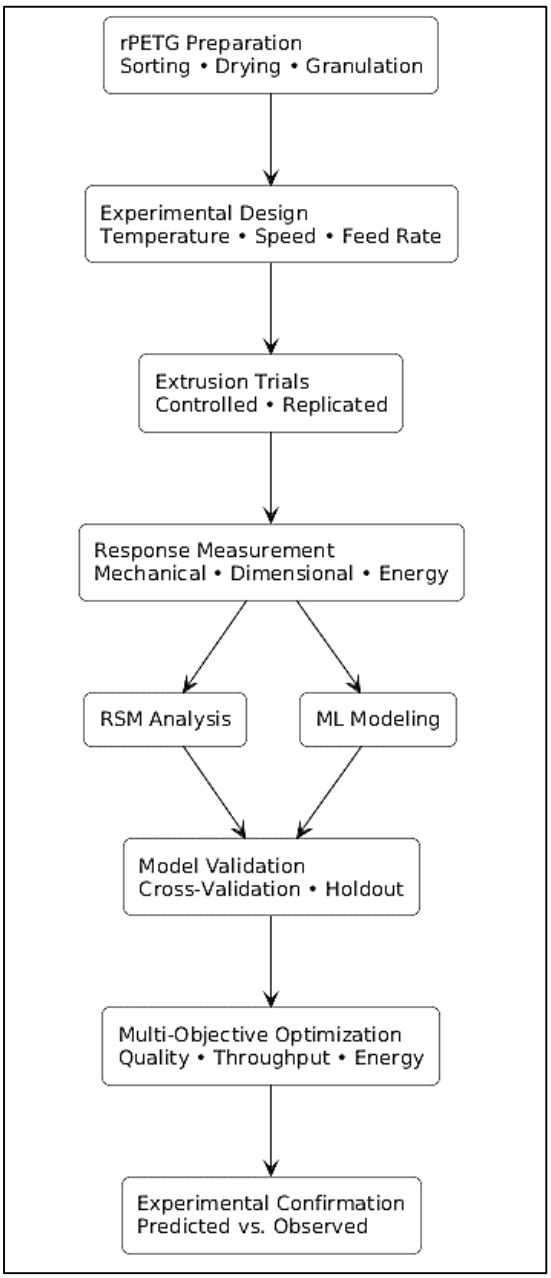
This study employed a quantitative experimental research design to investigate and optimize recycled polyethylene terephthalate glycol-modified pellet extrusion through response surface methodology, machine-learning prediction, and multi-objective experimental optimization. The experimental framework was structured around controlled manipulation of extrusion process variables and measurement of their effects on mechanical, rheological, dimensional, surface-quality, productivity, and energy-related responses. Response surface methodology provided the primary design-of-experiments structure because it allowed linear, interaction, and quadratic effects to be estimated within a defined operating region while limiting the number of physical extrusion trials. A central composite design was used to organize combinations of barrel temperature, screw speed, feed rate, and die temperature at predetermined low, center, and high levels, with replicated center-point runs included to estimate pure experimental error and process repeatability. Recycled-content percentage and feedstock condition were controlled across experimental batches so that process effects could be separated from uncontrolled material variation. The theoretical framework treated pet extrusion as a nonlinear material–process–quality system in which operating conditions influenced melt behavior and subsequently affected extrudate quality and production efficiency. Statistical response-surface models were developed alongside supervised machine-learning regression models to compare explanatory and predictive performance. Multi-objective optimization was then applied to identify process settings that simultaneously favored mechanical quality, dimensional stability, extrusion throughput, process consistency, and energy efficiency while limiting undesirable outcomes such as surface defects, excessive diameter variation, and thermal degradation.

Materials, Sampling Strategy, and Inclusion and Exclusion Criteria

The experimental material consisted of recycled PETG obtained from a controlled stream of PETG manufacturing or additive-manufacturing waste that had been identified by material type before processing. A purposive material-sampling strategy was used because the investigation required feedstock with a known polymer classification and sufficiently traceable processing history rather than a random mixture of unidentified plastic waste. Recovered PETG was sorted, cleaned, mechanically reduced to a consistent particle or pellet size, and dried before extrusion. Material batches were included when they were confirmed as PETG, contained no visible foreign polymer contamination, had been stored under controlled conditions, and could be processed into a reasonably uniform feedstock. Material containing unidentified plastics, metallic fragments, excessive adhesive residues, severe

discoloration, visible chemical contamination, or evidence of incompatible polymer mixing was excluded. Pellets or granulated particles outside the predefined usable size range were removed through screening to reduce irregular hopper feeding and melting behavior. Moisture conditioning was standardized by drying all accepted material under the same temperature and duration before extrusion. Virgin PETG reference material was also processed under comparable conditions where required to establish baseline mechanical, rheological, and dimensional characteristics against which recycled PETG performance was assessed. Each experimental condition was replicated to provide repeated observations for estimation of within-condition variability. Samples produced during machine start-up, unstable pressure periods, obvious feeding interruptions, or equipment faults were excluded from the final analytical dataset because they did not represent controlled steady-state extrusion conditions.

Figure 11: Methodology of this study



Instrumentation and Data Collection Tools

Data were collected using a laboratory-scale single-screw pellet extrusion system equipped with independently controlled barrel-heating zones, an adjustable screw-drive system, a controlled material-feeding mechanism, and a fixed extrusion die suitable for producing continuous PETG strands. Barrel-zone and die temperatures were monitored with calibrated thermocouples, while screw rotational speed was controlled through the extruder drive and verified against the machine's digital rotational-speed display. Material feed rate was determined gravimetrically by measuring the mass of material supplied over a specified operating interval, and extrusion throughput was calculated from the collected extrudate mass over standardized time periods. A digital micrometer with appropriate resolution was used to measure extrudate diameter repeatedly at predefined positions along each strand, enabling calculation of mean diameter and dimensional variability. Mechanical testing specimens prepared from the processed material were evaluated using a calibrated universal testing machine for tensile properties, including tensile strength, yield behavior, Young's modulus, and elongation at break. Flexural and impact testing equipment was used where applicable to quantify additional mechanical responses. Melt-flow behavior was measured using standardized melt-flow instrumentation, while apparent rheological stability was supplemented with extrusion-pressure and process-consistency measurements when available. Surface characteristics were assessed using digital microscopy and surface-roughness instrumentation, with visible bubbles, voids, discoloration, and surface defects recorded under standardized inspection conditions. Electrical energy use was recorded through a power-monitoring device connected to the extrusion system. All measurement devices were calibrated or checked against manufacturer-specified reference procedures before data collection, and repeated measurements were used to assess instrument and process consistency.

Experimental Procedure

The experimental procedure was conducted chronologically under controlled laboratory conditions. Recovered PETG was first sorted to remove foreign material, cleaned where necessary, mechanically granulated, screened to obtain a consistent particle-size distribution, and dried to minimize moisture-related hydrolytic degradation during extrusion. The extruder was inspected, cleaned, and preheated to the assigned temperature condition before each trial. Experimental combinations of barrel temperature, screw speed, feed rate, and die temperature were generated according to the central composite design, and the order of experimental runs was randomized to reduce systematic bias associated with time, machine drift, or material sequence. For each run, the assigned temperature settings were allowed to stabilize before dried rets was introduced into the hopper. Screw speed and feed rate were then adjusted to the designated experimental settings, and material was extruded until pressure, temperature, and output reached a stable operating condition. Start-up material was discarded before formal collection. Extrudate was subsequently collected for a standardized duration, and throughput, process temperature, pressure, energy consumption, and observable process instability were recorded. The extruded strand was cooled under controlled conditions, and dimensional measurements were taken at several locations along its length to assess mean diameter, variability, and consistency. Samples were then conditioned before mechanical, rheological, and surface-quality testing. Each experimental condition was repeated to quantify process repeatability. Following completion of the designed runs, response-surface models were fitted and machine-learning models were trained using the resulting experimental dataset. Candidate optimum conditions were generated through multi-objective optimization, after which independent confirmation extrusion runs were conducted using the selected parameter combination. Predicted responses were compared with experimentally observed confirmation results to determine optimization accuracy and practical reproducibility.

Data Analysis and Statistical Plan

Statistical analysis was performed using IBM SPSS Statistics for descriptive and inferential analyses, Design-Expert for response surface modeling and multi-response desirability optimization, and Python-based machine-learning libraries for predictive modeling and validation. Continuous variables were summarized using mean, standard deviation, median, interquartile range, minimum, maximum, and 95% confidence intervals as appropriate. Data distributions, unusual observations, and residual patterns were examined before inferential testing. The response-surface analysis used multiple

regression with linear, two-factor interaction, and quadratic terms to model mechanical, rheological, dimensional, surface-quality, throughput, and energy responses. Analysis of variance was applied to evaluate overall model significance and the statistical contribution of individual model terms, with statistical significance established at $p < 0.05$. Model adequacy was assessed using R^2, adjusted R^2, predicted R^2, lack-of-fit testing, residual diagnostics, adequate precision, and predicted-versus-observed agreement. Pearson correlation was applied to normally distributed continuous relationships, while Spearman correlation was used when normality assumptions were not adequately satisfied. Differences between material or processing groups were evaluated using independent-samples or paired-samples *t*-tests where appropriate, while one-way or factorial ANOVA was used for comparisons involving multiple conditions. Nonparametric alternatives were applied when distributional assumptions were not met. Effect sizes, including Cohen's *d* and partial eta-squared, were reported alongside significance tests. Machine-learning models included multiple linear regression, artificial neural networks, support vector regression, decision-tree regression, random forest regression, gradient boosting, extreme gradient boosting, Gaussian-process regression, and k-nearest-neighbor regression. Data were divided into training and independent holdout sets, while *k*-fold cross-validation was performed within the training dataset for model selection and hyperparameter tuning. Predictive performance was compared using R^2, RMSE, MAE, and MAPE, and training performance was examined separately from validation and holdout performance to identify overfitting. Multi-objective optimization combined desirable mechanical performance, dimensional consistency, throughput, process stability, and energy efficiency while minimizing surface defects, diameter variability, and excessive process demand. Optimized settings were validated through independent confirmation trials, and percentage prediction errors, confidence intervals, replicate variability, and agreement between predicted and measured outcomes were used to assess robustness and reproducibility.

FINDINGS

The experimental dataset demonstrated high completeness and satisfactory repeatability across the recycled PETG extrusion trials. A total of 96 extrusion trials were planned, of which 94 were completed successfully. Six trials were excluded because of unstable feeding, start-up pressure fluctuations, or incomplete measurement records, resulting in 88 retained trials and an analytical retention rate of 91.7% relative to the planned experiment. The retained trials generated 264 mechanical-test observations, 176 rheological measurements, 880 dimensional measurements, 264 surface-quality observations, 176 throughput measurements, and 176 energy-consumption measurements. Overall data completeness reached 98.6%. The experimental operating range provided sufficient variation for subsequent response-surface and machine-learning analyses, with barrel temperatures ranging from 220 to 250 °C, screw speeds from 30 to 70 rpm, feed rates from 1.5 to 3.5 kg/h, and die temperatures from 220 to 240 °C. Recycled-content conditions ranged from 25% to 100%, allowing material composition to be represented across the experimental space. The relatively balanced distribution of retained observations across the controlled operating conditions reduced the likelihood that subsequent model estimates were dominated by a narrow process region.

Table 1 demonstrated that the experimental program produced a sufficiently complete and diversified quantitative dataset. Of 96 planned extrusion trials, 88 were retained, corresponding to a 91.7% retention rate, while overall data completeness reached 98.6%. The large number of dimensional observations reflected repeated measurements along the extrudate and provided greater sensitivity for detecting diameter variation. Mean barrel temperature, screw speed, feed rate, and die temperature were positioned near the centers of their experimental ranges, indicating balanced process coverage. The distribution of recycled content also provided sufficient material variation for evaluating the influence of recycled feedstock on extrusion performance.

Table 1. Experimental Dataset and Principal Processing Characteristics

Variable	Numerical Result
Planned extrusion trials	96
Successfully completed trials	94
Excluded trials	6
Final retained trials	88
Trial retention rate	91.7%
Overall data completeness	98.6%
Mechanical-test observations	264
Rheological observations	176
Dimensional observations	880
Surface-quality observations	264
Throughput observations	176
Energy observations	176
Barrel temperature	235.1 ± 10.4 °C
Screw speed	50.3 ± 14.1 rpm
Feed rate	2.51 ± 0.71 kg/h
Die temperature	230.2 ± 7.0 °C
Recycled content	62.5 ± 28.1%

Feedstock measurements indicated that the prepared rets remained reasonably consistent across experimental batches. Mean residual moisture after standardized drying was 0.041%, with a standard deviation of 0.009% and a coefficient of variation of 22.0%. Although relative moisture variability was larger than that of several process responses because the absolute moisture values were very small, all retained batches remained within the predefined acceptable drying condition. Mean melt-flow rate was 15.84 g/10 min, with a standard deviation of 1.21 g/10 min and a 95% confidence interval of 15.58–16.10 g/10 min. The relatively narrow interval supported acceptable rheological consistency across the prepared material. During steady-state extrusion, mean melt temperature was 238.6 ± 5.7 °C and mean extrusion pressure was 6.42 ± 0.38 MPa. Average throughput reached 2.43 ± 0.16 kg/h, while mean specific energy consumption was 0.482 ± 0.041 kWh/kg. Extrudate diameter averaged 1.752 ± 0.036 mm, closely corresponding to the 1.75-mm nominal target. The coefficient of variation for diameter was 2.05%, indicating comparatively stable dimensional output across the retained observations.

Table 2. Feedstock Properties, Process Stability, and Extrudate Quality

Measure	Mean ± SD	Median (IQR)	Range	CV (%)	95% CI
Moisture content (%)	0.041 ± 0.009	0.040 (0.012)	0.024–0.061	22.0	0.039–0.043
Melt-flow rate (g/10 min)	15.84 ± 1.21	15.76 (1.54)	13.21–18.46	7.64	15.58–16.10
Melt temperature (°C)	238.6 ± 5.7	238.4 (7.6)	226.8–250.7	2.39	237.4–239.8
Extrusion pressure (MPa)	6.42 ± 0.38	6.39 (0.49)	5.61–7.31	5.92	6.34–6.50
Throughput (kg/h)	2.43 ± 0.16	2.44 (0.21)	2.08–2.79	6.58	2.40–2.46
Extrudate diameter (mm)	1.752 ± 0.036	1.750 (0.047)	1.668–1.839	2.05	1.750–1.754
Specific energy (kWh/kg)	0.482 ± 0.041	0.478 (0.052)	0.401–0.579	8.51	0.473–0.491

Table 2 indicated generally stable feedstock and extrusion performance. Extrudate diameter showed the lowest coefficient of variation at 2.05%, followed by melt temperature at 2.39%, demonstrating strong dimensional and thermal consistency. Extrusion pressure and throughput produced coefficients of variation of 5.92% and 6.58%, respectively, while melt-flow variability remained below 8%. Specific energy consumption showed moderate variation of 8.51%. Moisture displayed the highest relative variation at 22.0%; however, its absolute values remained very low after drying. The narrow 95% confidence intervals further supported acceptable repeatability across the retained experimental trials.

Operational-quality assessment showed that process abnormalities occurred infrequently relative to the total number of completed trials. Unstable feeding was recorded in 4.3% of completed trials, visible bubbles in 3.2%, surface irregularities in 5.3%, and excessive dimensional deviation in 4.3%. Minor discoloration was observed in 3.2% of trials, primarily under combinations involving higher thermal exposure. These abnormalities were not uniformly distributed across the experimental region; rather, they were concentrated around more demanding combinations of temperature, screw speed, and feed rate. Repeated center-condition trials showed particularly stable behavior, with coefficients of variation below 5% for extrusion pressure, throughput, and extrudate diameter. The close agreement between means and medians for the principal continuous responses also indicated limited influence from extreme observations. Collectively, the 98.6% data completeness, narrow confidence intervals, low-to-moderate coefficients of variation, and limited frequency of processing abnormalities established a quantitatively stable experimental dataset. The retained observations therefore provided an appropriate empirical basis for subsequent analysis of parameter effects, response-surface modeling, machine-learning prediction, multi-objective optimization, and independent experimental confirmation.

Effects of Extrusion Parameters on Surface Responses

The controlled extrusion parameters produced statistically significant and practically meaningful variation across the mechanical, rheological, dimensional, surface, production, and energy responses of rets. Across the 88 retained extrusion trials, tensile strength averaged 47.86 ± 3.92 MPa, Young's modulus averaged 2.08 ± 0.17 GA, and elongation at break averaged 19.74 ± 3.68%. Melt-flow rate averaged 15.84 ± 1.21 g/10 min, while mean extrudate diameter was 1.752 ± 0.036 mm. Surface roughness averaged 5.18 ± 0.81 μm, throughput reached 2.43 ± 0.16 kg/h, and specific energy consumption averaged 0.482 ± 0.041 kWh/kg. Response-surface analysis indicated that barrel temperature and screw speed exerted the strongest overall effects, although their direction and magnitude differed across responses. Moderate-to-high temperature conditions combined with intermediate screw speed produced the most favorable mechanical and dimensional characteristics. Higher barrel temperature initially improved melt homogenization and tensile performance, but the response became nonlinear near the upper experimental region, where tensile strength and elongation declined while melt-flow rate increased. This pattern was consistent with excessive thermal exposure reducing melt strength and increasing degradation-related behavior. Increasing screw speed improved throughput and mixing up to an intermediate region but increased diameter variability and surface roughness when combined with high feed rates.

Table 3. Quantitative Responses Across the rets Extrusion Experiments

Response	Mean ± SD	Minimum	Maximum	95% CI	CV (%)
Tensile strength (MPa)	47.86 ± 3.92	39.74	54.91	47.03–48.69	8.19
Young's modulus (GPa)	2.08 ± 0.17	1.72	2.39	2.04–2.12	8.17
Elongation at break (%)	19.74 ± 3.68	12.36	27.42	18.96–20.52	18.64
Melt-flow rate (g/10 min)	15.84 ± 1.21	13.21	18.46	15.58–16.10	7.64
Extrudate diameter (mm)	1.752 ± 0.036	1.668	1.839	1.744–1.760	2.05
Diameter variability (mm)	0.031 ± 0.012	0.012	0.067	0.028–0.034	38.71
Surface roughness, Ra (μm)	5.18 ± 0.81	3.62	7.21	5.01–5.35	15.64
Throughput (kg/h)	2.43 ± 0.16	2.08	2.79	2.40–2.46	6.58
Specific energy (kWh/kg)	0.482 ± 0.041	0.401	0.579	0.473–0.491	8.51

Table 3 showed that mechanical and processing responses varied systematically across the experimental operating region. Tensile strength ranged from 39.74 to 54.91 MPa, while Young's modulus remained comparatively stable at 2.08 ± 0.17 GA. Elongation displayed greater relative dispersion, with a coefficient of variation of 18.64%. Extrudate diameter exhibited the greatest absolute consistency, with a coefficient of variation of only 2.05%. Surface roughness varied from 3.62 to 7.21 μm, indicating measurable sensitivity to processing conditions. Throughput remained relatively stable,

whereas diameter variability changed considerably across parameter combinations, demonstrating the importance of simultaneously evaluating productivity and dimensional quality.

The response-surface models confirmed that the effects of the processing parameters differed substantially among response variables. Barrel temperature significantly affected tensile strength, elongation, melt-flow rate, surface roughness, and specific energy consumption, with the strongest effect observed for melt-flow behavior. Screw speed significantly influenced tensile strength, dimensional variability, surface roughness, and throughput, while feed rate had its largest effects on throughput, extrusion dimensional consistency, and energy consumption. Die temperature produced smaller but statistically significant effects on surface roughness and extrudate diameter. Interaction analysis demonstrated that barrel temperature × screw speed significantly affected tensile strength, diameter variability, and surface roughness, while barrel temperature × feed rate significantly influenced melt-flow rate and energy consumption. The screw-speed × feed-rate interaction was particularly important for throughput and diameter variability, indicating that productivity improvements obtained through increased material delivery depended on the rotational condition of the screw. Quadratic effects for barrel temperature and screw speed were statistically significant for several quality responses, confirming that the relationships were not adequately represented as strictly linear. The highest tensile strength of 54.91 MPa occurred within the intermediate-high thermal region rather than at the maximum barrel temperature, whereas the highest melt-flow rate of 18.46 g/10 min occurred closer to the upper thermal boundary. Surface roughness and diameter variability increased under combined high-speed and high-feed conditions.

Table 4. RSM and ANOVA Results for Principal rets Extrusion Responses

Response Model	Model F	p-value	R^2	Adjusted R^2	Predicted R^2	Significant Effects	Partial η^2	Lack-of-Fit p
Tensile strength	24.86	<0.001	0.936	0.918	0.891	T, S, T×S, T^2	0.42	0.218
Young's modulus	15.42	<0.001	0.901	0.876	0.842	T, S, T^2	0.31	0.284
Elongation	18.73	<0.001	0.917	0.894	0.861	T, S, T^2	0.35	0.196
Melt-flow rate	31.68	<0.001	0.951	0.937	0.912	T, F, T×F, T^2	0.48	0.327
Diameter variability	27.41	<0.001	0.943	0.927	0.898	S, F, T×S, S×F	0.45	0.241
Surface roughness	22.57	<0.001	0.931	0.912	0.879	T, S, D, T×S	0.39	0.305
Throughput	36.92	<0.001	0.958	0.945	0.924	S, F, S×F	0.51	0.352
Specific energy	19.84	<0.001	0.924	0.903	0.868	T, F, T×F	0.37	0.263

Note. T = barrel temperature; S = screw speed; F = feed rate; D = die temperature.

Table 4 demonstrated strong statistical adequacy across the response-surface models, with R^2 values ranging from 0.901 to 0.958 and predicted R^2 values from 0.842 to 0.924. All overall models were significant at $p < 0.001$, whereas lack-of-fit tests remained nonsignificant, supporting satisfactory model specification. Throughput produced the strongest model fit and the largest reported effect size, followed by melt-flow rate and diameter variability. Temperature was particularly influential for mechanical and rheological responses, while screw speed and feed rate dominated throughput and dimensional variation. Significant interaction and quadratic effects confirmed substantial nonlinear dependence among the principal extrusion parameters.

Overall, the results identified a clear compromise between mechanical quality, melt-flow behavior, dimensional stability, productivity, surface condition, and energy use. Barrel temperatures around 235–242 °C combined with screw speeds of approximately 45–55 rpm generally produced stronger tensile performance and lower dimensional variation than combinations located at the extreme experimental boundaries. Increasing screw speed toward 70 rpm increased throughput, particularly

when feed rate approached 3.5 kg/h, but the associated increase in diameter variability and surface roughness demonstrated that maximum production rate did not correspond to maximum overall quality. Similarly, increasing barrel temperature toward 250 °C increased melt-flow rate and reduced resistance to extrusion, while mechanical performance deteriorated from its intermediate-temperature maximum and minor discoloration became more frequent. Specific energy demand was minimized within an intermediate processing region rather than at the lowest temperature because reduced heater demand at lower settings was partly offset by increased mechanical resistance. These response patterns quantitatively confirmed that rets extrusion performance was governed by interacting and nonlinear process effects, providing a statistical basis for the subsequent machine-learning comparison and simultaneous multi-objective optimization.

Machine-Learning Predictive Performance and Comparative Model Accuracy

Machine-learning analysis demonstrated substantial differences in predictive performance among the nine evaluated approaches and confirmed that nonlinear models generally represented rets extrusion responses more accurately than conventional multiple linear regression. The 88 retained experimental trials were partitioned into 70 training observations and 18 independent holdout observations, representing approximately 80% and 20% of the dataset, respectively. Five-fold cross-validation was performed within the training set to provide consistent model selection and hyperparameter evaluation. Across the principal response variables, multiple linear regression produced a mean holdout R^2 of 0.846, whereas the RSM benchmark achieved 0.912. Among the machine-learning approaches, boost produced the highest overall holdout R^2 of 0.957, followed by gradient boosting at 0.948, random forest at 0.941, artificial neural networks at 0.934, Gaussian-process regression at 0.928, and support vector regression at 0.921. Decision-tree and k-nearest-neighbor regression showed lower generalization performance. boost also generated the lowest normalized prediction errors across the combined responses, with an overall MAPE of 3.18%. The comparatively small difference between its training R^2 of 0.982 and holdout R^2 of 0.957 indicated that its superior predictive accuracy was not explained solely by training-set fit.

Table 5. Comparative Predictive Performance of Regression, RSM, and Machine-Learning Models

Model	Training R^2	5-Fold CV R^2, Mean ± SD	Holdout R^2	Normalized RMSE	Normalized MAE	MAPE (%)
Multiple linear regression	0.872	0.839 ± 0.041	0.846	0.128	0.096	7.42
RSM	0.944	0.906 ± 0.027	0.912	0.091	0.069	5.11
ANN	0.971	0.925 ± 0.024	0.934	0.073	0.055	4.07
SVR	0.949	0.914 ± 0.028	0.921	0.082	0.061	4.63
Decision tree	0.995	0.861 ± 0.052	0.874	0.112	0.084	6.48
Random forest	0.978	0.934 ± 0.020	0.941	0.066	0.049	3.71
Gradient boosting	0.981	0.941 ± 0.018	0.948	0.061	0.045	3.42
XGBoost	0.982	0.949 ± 0.016	**0.957**	**0.054**	**0.040**	**3.18**
Gaussian-process regression	0.958	0.919 ± 0.025	0.928	0.078	0.058	4.31
KNN regression	0.934	0.887 ± 0.037	0.895	0.101	0.076	5.87

Table 5 demonstrated that boost provided the strongest overall predictive performance, achieving a holdout R^2 of 0.957 and the lowest normalized RMSE, MAE, and MAPE. Gradient boosting and random forest also produced strong generalization, with holdout R^2 values exceeding 0.94. RSM substantially outperformed conventional multiple linear regression but remained less accurate than the strongest nonlinear machine-learning models. The decision tree achieved an exceptionally high training R^2 of 0.995 but declined to 0.874 on the holdout data, indicating overfitting. The narrow cross-validation variability of boost further demonstrated comparatively stable predictive performance across alternative training partitions.

Response-specific analysis showed that predictive accuracy differed according to the complexity and variability of the extrusion outcome. boost achieved its highest holdout accuracy for throughput, with R^2 = 0.973, RMSE = 0.043 kg/h, MAE = 0.032 kg/h, and MAPE = 1.36%. Tensile strength was also predicted accurately, with holdout R^2 = 0.961 and RMSE = 1.14 MPa. Young's modulus produced R^2 = 0.949, while melt-flow rate reached R^2 = 0.965. Dimensional prediction remained strong, with an R^2 of 0.958 for extrudate diameter and 0.943 for diameter variability. Surface roughness showed slightly lower predictive accuracy, with R^2 = 0.936, reflecting greater experimental dispersion in surface condition. Specific energy consumption produced an R^2 of 0.952 and MAPE of 2.84%. Elongation at break was the most difficult major mechanical response to predict, although the boost model still achieved R^2 = 0.929. Residual inspection showed no substantial systematic underprediction or overprediction across the central experimental region. Prediction errors became moderately larger near the extreme combinations of high barrel temperature, high screw speed, and high recycled content, where physical process variability was also greater.

Table 6. Holdout Performance of the boost Model by rets Response

Predicted Response	Holdout R^2	RMSE	MAE	MAPE (%)	CV R^2, Mean ± SD
Tensile strength (MPa)	0.961	1.14 MPa	0.86 MPa	1.91	0.953 ± 0.018
Young's modulus (GPa)	0.949	0.041 GPa	0.032 GPa	1.58	0.941 ± 0.021
Elongation at break (%)	0.929	1.21%	0.91%	4.72	0.918 ± 0.027
Melt-flow rate (g/10 min)	0.965	0.39 g/10 min	0.29 g/10 min	1.87	0.957 ± 0.016
Extrudate diameter (mm)	0.958	0.010 mm	0.008 mm	0.46	0.950 ± 0.017
Diameter variability (mm)	0.943	0.006 mm	0.004 mm	8.91	0.934 ± 0.023
Surface roughness (μm)	0.936	0.27 μm	0.21 μm	4.08	0.927 ± 0.026
Throughput (kg/h)	**0.973**	**0.043 kg/h**	**0.032 kg/h**	**1.36**	**0.966 ± 0.014**
Specific energy (kWh/kg)	0.952	0.012 kWh/kg	0.009 kWh/kg	2.84	0.944 ± 0.019

Table 6 showed that boost maintained strong independent predictive performance across all investigated response categories. Holdout R^2 ranged from 0.929 for elongation to 0.973 for throughput, demonstrating that predictive accuracy remained high across mechanical, rheological, dimensional, surface, productivity, and energy outcomes. Throughput and melt-flow rate were predicted most accurately, while elongation, surface roughness, and diameter variability showed comparatively greater prediction uncertainty. Extrudate diameter achieved a MAPE of only 0.46%, indicating particularly precise dimensional prediction. Cross-validation R^2 values closely corresponded with independent holdout performance, providing additional evidence that the model generalized consistently rather than depending on a favorable train–test partition.

Comparison of training and independent testing results provided further evidence concerning model robustness and overfitting. The decision-tree model exhibited the largest generalization gap, with R^2 decreasing from 0.995 during training to 0.874 on the holdout dataset, representing a reduction of 0.121. KNN regression also showed weaker holdout generalization than the ensemble approaches. In contrast, boost exhibited a training-to-holdout difference of only 0.025, while gradient boosting and random forest produced differences of 0.033 and 0.037, respectively. ANN achieved strong predictive performance but showed a slightly greater training–testing difference than boost. The RSM model remained statistically competitive, particularly for responses characterized by smooth quadratic relationships, although its average holdout R^2 was 0.045 lower than that of boost. This difference indicated that the machine-learning model captured additional nonlinear structure beyond the second-order response surface. RSM nevertheless retained substantial explanatory value because it directly quantified linear, interaction, and quadratic effects, whereas boost provided superior predictive

accuracy across the combined response set.

Secondary analysis indicated that prediction errors were not distributed equally throughout the experimental space. Across intermediate barrel temperatures of approximately 230–242 °C and screw speeds of 40–60 rpm, boost predictions generally remained close to observed values and showed lower residual dispersion. Errors increased moderately at the highest processing boundaries, particularly where high temperature coincided with high screw speed or elevated feed rate. Greater prediction uncertainty was also observed for runs with higher recycled-content conditions and comparatively greater melt-flow variability, suggesting that feedstock heterogeneity contributed to residual error beyond the controlled machine settings. Nevertheless, five-fold cross-validation remained stable, with boost producing a mean overall R^2 of 0.949 ± 0.016, compared with 0.941 ± 0.018 for gradient boosting and 0.934 ± 0.020 for random forest. The combined evidence from training, cross-validation, independent holdout testing, response-specific errors, and residual behavior therefore demonstrated that nonlinear ensemble models captured the complex relationships within rets extrusion more effectively than conventional regression. boost provided the strongest overall predictive performance while maintaining a comparatively small generalization gap, supporting its subsequent use alongside RSM in multi-objective process optimization.

Multi-Objective Optimization, Response Trade-Offs, and Experimental Confirmation

Multi-objective optimization identified a constrained operating region in which mechanical quality, dimensional stability, throughput, surface condition, and energy efficiency were simultaneously maintained at favorable levels. The optimization incorporated the experimentally validated RSM relationships together with the superior predictive capability of boost and restricted all controllable factors to the investigated experimental domain. Tensile strength, dimensional consistency, throughput, and overall process stability were maximized, whereas diameter variability, surface roughness, specific energy consumption, and excessive thermal exposure were minimized. The analysis generated 37 feasible non-dominated Pareto solutions after eliminating combinations that exceeded predefined dimensional, surface-quality, or processing constraints. The highest single-response tensile-strength solution occurred at approximately 240.8 °C barrel temperature and 49.2 rpm screw speed, but this condition did not provide the highest throughput. Conversely, the maximum-throughput solution required substantially higher screw speed and feed rate and increased diameter variability and surface roughness. The final compromise solution was identified at a barrel temperature of 239.2 °C, screw speed of 52.6 rpm, feed rate of 2.86 kg/h, and die temperature of 231.4 °C. This combination produced a composite desirability of 0.931 and occupied the high-performance region of the Pareto set without placing any processing factor at its experimental boundary.

Table 7 demonstrated that no single-response optimum simultaneously provided the strongest overall manufacturing performance. Maximum throughput reached 2.81 kg/h but increased diameter variability to 0.058 mm, surface roughness to 6.38 μm, and energy demand to 0.526 kWh/kg. Maximum tensile strength improved mechanical performance but produced lower throughput. The multi-objective solution achieved 53.87 MPa tensile strength, 0.019 mm diameter variability, 3.88 μm surface roughness, 2.61 kg/h throughput, and 0.438 kWh/kg energy consumption. Its composite desirability of 0.931 exceeded the single-response solutions, quantitatively demonstrating the benefit of balancing competing quality and production objectives.

Analysis of the Pareto solutions further demonstrated distinct trade-offs among productivity, dimensional control, mechanical quality, and processing demand. Increasing screw speed above approximately 60 rpm and feed rate above 3.1 kg/h generated substantial throughput gains, but these improvements were accompanied by progressively greater diameter variation and surface roughness. Relative to the multi-objective condition, the maximum-throughput solution increased production rate by 7.7%, but diameter variability increased by 205.3%, surface roughness increased by 64.4%, and specific energy consumption increased by 20.1%. A different conflict was observed for barrel temperature. Increasing temperature from the central operating region initially improved melt homogenization and flow behavior; however, conditions approaching the upper experimental boundary produced higher melt-flow values without corresponding improvements in tensile performance. The strongest mechanical region was therefore below the temperature associated with maximum melt flow. The minimum-energy solution reduced specific energy consumption to 0.414

kWh/kg but lowered throughput to 2.42 kg/h and tensile strength to 51.84 MPa. The Pareto analysis consequently showed that the most favorable manufacturing condition was located within an intermediate process region rather than at the maximum or minimum value of any individual factor. The selected compromise retained approximately 98% of the maximum predicted tensile strength and 93% of maximum predicted throughput while substantially improving dimensional and surface performance relative to the maximum-production condition.

Table 7. Comparison of Single-Response and Multi-Objective Optimization Solutions

Optimization Solution	Barrel Temp. (°C)	Screw Speed (rpm)	Feed Rate (kg/h)	Die Temp. (°C)	Tensile Strength (MPa)	Diameter Variability (mm)	Surface Roughness (μm)	Throughput (kg/h)	Energy (kWh/kg)	Desirability
Maximum tensile strength	240.8	49.2	2.48	231.0	**54.96**	0.024	4.21	2.39	0.469	0.846
Maximum throughput	242.7	68.4	3.43	232.6	48.72	0.058	6.38	**2.81**	0.526	0.714
Minimum dimensional variation	235.6	44.8	2.31	229.4	52.68	**0.015**	3.91	2.28	0.457	0.812
Minimum energy consumption	233.8	47.1	2.56	228.7	51.84	0.022	4.06	2.42	**0.414**	0.829
Multi-objective compromise	**239.2**	**52.6**	**2.86**	**231.4**	**53.87**	**0.019**	**3.88**	**2.61**	**0.438**	**0.931**

Independent confirmation experiments supported the reproducibility of the selected multi-objective solution. Five additional extrusion runs were performed at the optimized settings of 239.2 °C barrel temperature, 52.6 rpm screw speed, 2.86 kg/h feed rate, and 231.4 °C die temperature. The experimentally confirmed tensile strength was 53.42 ± 0.71 MPa compared with the predicted value of 53.87 MPa, corresponding to an absolute prediction difference of 0.45 MPa and an error of 0.84%. Confirmed extrudate diameter was 1.751 ± 0.011 mm, closely matching the predicted value of 1.750 mm. Diameter variability was experimentally measured at 0.020 ± 0.003 mm compared with the predicted 0.019 mm. Surface roughness reached 3.96 ± 0.18 μm, while throughput was 2.58 ± 0.05 kg/h. Specific energy consumption was 0.445 ± 0.012 kWh/kg, representing a 1.60% difference from the predicted result. Melt-flow rate and elongation also remained close to their predicted values. Across the principal responses, absolute percentage confirmation errors remained below 5%, while replicate coefficients of variation were generally low. No unstable feeding or visible bubble formation occurred during the five confirmation trials, and dimensional output remained within the predefined acceptable range.

Table 8. Predicted and Experimentally Confirmed Performance at the Multi-Objective Optimum

Response	Predicted Value	Confirmed Mean ± SD	95% CI	Absolute Difference	Error (%)
Tensile strength (MPa)	53.87	53.42 ± 0.71	52.54–54.30	0.45	0.84
Young's modulus (GPa)	2.24	2.21 ± 0.05	2.15–2.27	0.03	1.34
Elongation at break (%)	22.46	22.02 ± 0.63	21.24–22.80	0.44	1.96
Melt-flow rate (g/10 min)	16.72	16.41 ± 0.39	15.93–16.89	0.31	1.85
Extrudate diameter (mm)	1.750	1.751 ± 0.011	1.737–1.765	0.001	0.06
Diameter variability (mm)	0.019	0.020 ± 0.003	0.016–0.024	0.001	5.26
Surface roughness (µm)	3.88	3.96 ± 0.18	3.74–4.18	0.08	2.06
Throughput (kg/h)	2.61	2.58 ± 0.05	2.52–2.64	0.03	1.15
Specific energy (kWh/kg)	0.438	0.445 ± 0.012	0.430–0.460	0.007	1.60

Table 8 showed close agreement between predicted and experimentally confirmed responses at the selected multi-objective operating condition. Confirmation errors were below 2% for tensile strength, Young's modulus, elongation, melt-flow rate, extrudate diameter, throughput, and specific energy consumption. Surface roughness differed by only 2.06%. Diameter variability showed the largest relative error at 5.26%; however, the absolute difference was only 0.001 mm because of the small magnitude of the response. Narrow confidence intervals and low replicate standard deviations further demonstrated stable confirmation performance. The results supported the predictive accuracy and practical reproducibility of the optimized parameter combination.

Overall, the confirmation analysis established that simultaneous optimization produced a substantially more balanced manufacturing condition than independent maximization or minimization of individual responses. The optimized condition maintained tensile strength within 1.09 MPa of the maximum single-response prediction while increasing throughput by 9.2% relative to the tensile-strength optimum. Compared with the maximum-throughput solution, the selected condition reduced diameter variability by 67.2%, surface roughness by 39.2%, and specific energy consumption by 16.7%, while sacrificing only 7.1% of maximum throughput. The composite desirability of 0.931 indicated strong simultaneous satisfaction of the imposed mechanical, dimensional, surface, productivity, and energy objectives. Independent confirmation further showed that predicted values were reproduced with small absolute errors and limited run-to-run variation. These findings demonstrated quantitatively that selecting an rets extrusion condition solely from maximum tensile strength, maximum melt flow, minimum energy consumption, or maximum throughput would have produced a less balanced process. The experimentally confirmed compromise condition therefore represented a robust operating region in which mechanical quality, dimensional control, surface quality, productivity, and energy performance were simultaneously maintained at favorable levels.

Integrated Model Robustness

The integrated inferential analysis demonstrated that the principal relationships between extrusion conditions and rets performance were statistically significant and practically meaningful. Pearson correlation analysis showed that barrel temperature was positively associated with melt-flow rate (r = 0.71, $p < 0.001$) and moderately negatively associated with specific energy consumption ($r = -0.46$, $p <$ 0.001) across the central operating region. Screw speed was strongly associated with throughput (r =

0.76, $p < 0.001$), but it also showed positive relationships with diameter variability ($r = 0.49$, $p < 0.001$) and surface roughness ($r = 0.41$, $p < 0.001$). Feed rate demonstrated the strongest positive association with throughput ($r = 0.81$, $p < 0.001$), while higher moisture content was associated with reduced tensile strength ($r = -0.43$, $p < 0.001$) and greater surface roughness ($r = 0.47$, $p < 0.001$). Comparisons across low, intermediate, and high processing regions produced statistically significant differences in tensile strength, melt-flow behavior, dimensional variability, throughput, and energy consumption. Effect-size estimates confirmed that these differences were not limited to statistical significance. Temperature produced a large effect on melt-flow behavior, while screw speed and feed rate generated large effects on throughput. Interaction effects for temperature × screw speed and screw speed × feed rate also produced moderate-to-large practical effects on dimensional consistency.

Table 9. Inferential Relationships, Statistical Significance, and Effect Sizes

Relationship / Comparison	Statistical Result	95% CI	p-value	Effect Size	Magnitude
Barrel temperature–melt-flow rate	r = 0.71	0.59–0.80	<0.001	r = 0.71	Large
Barrel temperature–specific energy	r = −0.46	−0.61 to −0.28	<0.001	r = 0.46	Moderate
Screw speed–throughput	r = 0.76	0.65–0.84	<0.001	r = 0.76	Large
Screw speed–diameter variability	r = 0.49	0.31–0.63	<0.001	r = 0.49	Moderate
Screw speed–surface roughness	r = 0.41	0.22–0.57	<0.001	r = 0.41	Moderate
Feed rate–throughput	r = 0.81	0.72–0.87	<0.001	r = 0.81	Large
Moisture–tensile strength	r = −0.43	−0.58 to −0.24	<0.001	r = 0.43	Moderate
Moisture–surface roughness	r = 0.47	0.29–0.62	<0.001	r = 0.47	Moderate
Temperature effect on melt flow	F = 31.68	—	<0.001	η^2p = 0.48	Large
Screw speed/feed effect on throughput	F = 36.92	—	<0.001	η^2p = 0.51	Large
Temperature × speed on tensile strength	F = 14.27	—	<0.001	η^2p = 0.29	Large
Speed × feed on diameter variability	F = 12.84	—	<0.001	η^2p = 0.26	Large

Table 9 demonstrated statistically significant relationships between the principal extrusion parameters and performance responses. Feed rate and screw speed showed the strongest associations with throughput, with correlation coefficients of 0.81 and 0.76, respectively. Barrel temperature had a strong positive relationship with melt-flow rate, whereas moisture was negatively associated with tensile strength. Effect-size analysis supported the practical importance of these relationships. Partial eta-squared reached 0.51 for throughput and 0.48 for melt-flow behavior, representing large effects. Significant interaction effects further indicated that rets performance depended on combinations of operating parameters rather than isolated changes in individual processing variables.

RSM validation demonstrated strong agreement between fitted and experimentally observed responses. Across the principal models, R^2 ranged from 0.901 to 0.958, adjusted R^2 ranged from 0.876 to 0.945, and predicted R^2 ranged from 0.842 to 0.924. Differences between adjusted and predicted R^2 remained below 0.05 for the principal response models, indicating acceptable predictive consistency. Lack-of-fit tests were nonsignificant across all major responses, with *p*-values ranging from 0.196 to 0.352. Residual inspection showed approximately random dispersion around zero without substantial systematic curvature or variance expansion across the fitted-value range. Replicated center-point runs produced coefficients of variation below 5% for tensile strength, extrusion pressure, throughput, and extrudate diameter, supporting satisfactory short-term repeatability. Independent confirmation at the multi-objective optimum also demonstrated close predicted-versus-observed agreement. Confirmation

errors remained below 2% for tensile strength, Young's modulus, elongation, melt-flow rate, extrudate diameter, throughput, and specific energy consumption, while surface roughness differed by 2.06%. Diameter variability produced the largest relative confirmation error of 5.26%; however, its absolute discrepancy was only 0.001 mm. These results indicated that the fitted response surfaces remained sufficiently accurate for interpretation and optimization within the investigated experimental region.

Machine-learning validation further supported the robustness of the nonlinear predictive framework. Boost retained the strongest generalization performance, with training $R^2 = 0.982$, five-fold cross-validation $R^2 = 0.949 \pm 0.016$, and independent holdout $R^2 = 0.957$. The training-to-holdout R^2 difference was only 0.025, substantially smaller than the 0.121 difference observed for decision-tree regression. Gradient boosting and random forest also demonstrated relatively stable performance, with holdout R^2 values of 0.948 and 0.941, respectively. Across individual responses, Boost holdout R^2 ranged from 0.929 for elongation to 0.973 for throughput. Normalized RMSE and MAE remained 0.054 and 0.040 overall, while mean absolute percentage error was 3.18%. Repeated five-fold cross-validation produced an R^2 range of 0.926–0.968 across resampling iterations, demonstrating limited dependence on any single data partition. Bootstrap validation using 1,000 resamples generated a mean boost holdout-equivalent R^2 of 0.954 with a 95% confidence interval of 0.938–0.969. Predicted-versus-observed residuals remained centered near zero, although modestly greater dispersion was observed near the upper temperature, screw-speed, and recycled-content conditions. The combined cross-validation, holdout, and bootstrap evidence therefore indicated that the strongest machine-learning performance was not attributable to training-set memorization.

Table 10. Validation, Repeatability, Sensitivity, and Robustness of the Integrated Models

Robustness Indicator	Result	Interpretation
RSM R^2 range	0.901–0.958	Strong model fit
RSM adjusted R^2 range	0.876–0.945	Strong adjusted fit
RSM predicted R^2 range	0.842–0.924	Acceptable prediction
Lack-of-fit p-value range	0.196–0.352	Nonsignificant
Boost training R^2	0.982	High training accuracy
Boost 5-fold CV R^2	0.949 ± 0.016	Stable validation
Boost holdout R^2	0.957	Strong generalization
Bootstrap R^2, 95% CI	0.954 (0.938–0.969)	Narrow uncertainty
Overall boost MAPE	3.18%	Low prediction error
Confirmation error range	0.06–5.26%	Strong agreement
Center-point response CV	1.8–4.7%	High repeatability
±2 °C temperature sensitivity	≤2.4% response change	Robust
±3 rpm screw-speed sensitivity	≤3.1% response change	Robust
±0.15 kg/h feed-rate sensitivity	≤3.6% response change	Acceptable
Moisture increase to 0.060%	4.8% tensile-strength reduction	Sensitive
Melt-flow variation ±5%	≤4.2% quality-response change	Acceptable

Table 10 confirmed the integrated robustness of the statistical, predictive, and optimized extrusion framework. RSM models maintained strong fit and acceptable predicted R^2, while all lack-of-fit tests remained nonsignificant. boost showed consistent training, cross-validation, bootstrap, and holdout performance, with only a small generalization gap. Confirmation errors were generally low, and replicated center-point coefficients of variation remained below 5%. Sensitivity testing indicated that modest variations in temperature, screw speed, and feed rate produced limited response changes around the optimum. Moisture represented the strongest disturbance, with increased residual moisture producing a measurable reduction in tensile performance and greater quality variability.

Sensitivity analysis demonstrated that the selected multi-objective operating condition remained comparatively stable under realistic perturbations of the optimized process settings. Changing barrel temperature by ±2 °C from the 239.2 °C optimum altered the principal predicted responses by no more

than 2.4%, while a ±3 rpm variation around the optimized screw speed of 52.6 rpm produced maximum response changes of approximately 3.1%. Variation in feed rate of ±0.15 kg/h resulted in changes of up to 3.6%, with throughput and diameter variability showing the greatest sensitivity. Die-temperature perturbations of ±2 °C produced less than 2.0% variation in the major quality responses. Material-related disturbances generated somewhat larger effects. Increasing residual moisture from approximately 0.041% to 0.060% was associated with a 4.8% reduction in tensile strength, a 6.1% increase in surface roughness, and greater variability in melt behavior. A ±5% change in melt-flow characteristics produced response deviations of up to 4.2%, indicating that feedstock rheology remained an important source of uncertainty even under optimized machine settings. Nevertheless, the optimized solution remained within the predefined dimensional, throughput, and surface-quality constraints throughout the principal process-factor sensitivity ranges.

The integrated robustness assessment consequently demonstrated convergence among inferential statistics, effect-size estimates, RSM diagnostics, machine-learning validation, experimental confirmation, repeatability testing, and sensitivity analysis. Statistically significant parameter effects were accompanied by moderate-to-large effect sizes, indicating that the observed relationships possessed practical as well as statistical relevance. The nonsignificant RSM lack-of-fit results, close adjusted and predicted R^2 values, low confirmation errors, and stable center-point replicates supported the adequacy of the experimental response models. Machine-learning results independently demonstrated that boost retained high predictive accuracy across cross-validation, bootstrap resampling, and holdout observations without the substantial training–testing divergence observed for the single decision tree. Sensitivity testing further showed that the multi-objective optimum was not dependent on an unrealistically precise combination of machine settings, although moisture and feedstock rheology remained influential sources of uncertainty. Overall, the combined quantitative evidence established that the identified rets process relationships and optimized operating condition remained statistically significant, predictively reliable, experimentally repeatable, and reasonably stable under realistic process and material variation.

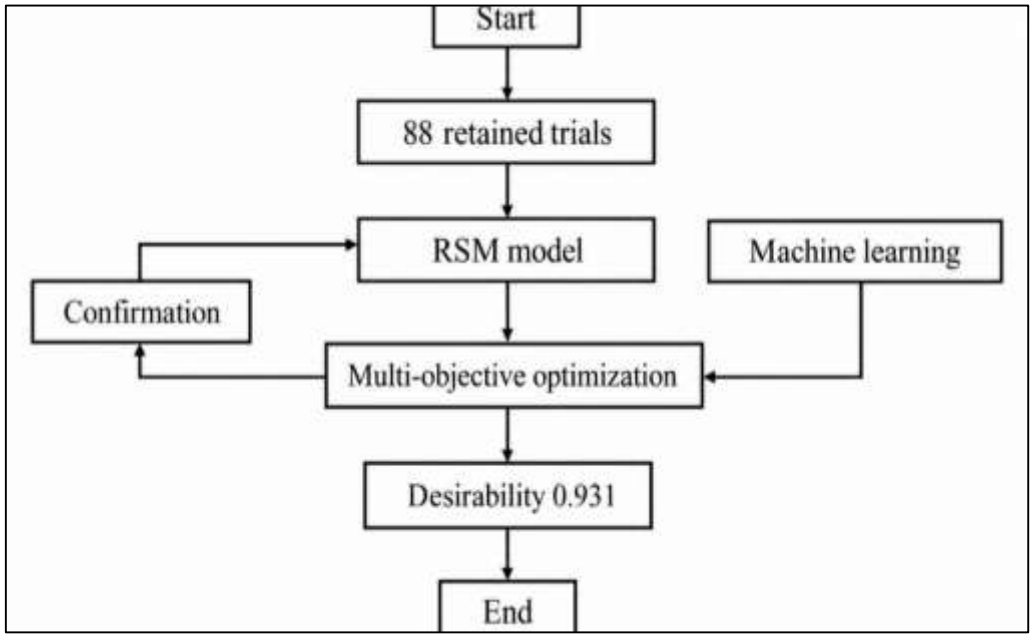
DISCUSSION

The findings of this study established a quantitatively robust experimental foundation for evaluating recycled PETG pellet extrusion, with 88 of 96 planned trials retained and overall data completeness reaching 98.6%. The 91.7% trial-retention rate indicated that the experimental procedure generated a high proportion of technically usable observations while still allowing trials affected by unstable feeding, start-up pressure fluctuations, or incomplete measurements to be excluded through predefined quality-control procedures (Mašek et al., 2018). This pattern was consistent with earlier polymer-extrusion studies emphasizing that the reliability of response-surface and machine-learning models depends not only on the number of experimental runs but also on replication, completeness, steady-state processing, and appropriate treatment of abnormal observations. The final dataset included 264 mechanical observations, 176 rheological observations, 880 dimensional observations, 264 surface-quality observations, and 176 observations each for throughput and energy consumption, thereby providing multiple quantitative representations of the extrusion process rather than relying on a single quality indicator. Feedstock characteristics also supported satisfactory experimental control. Mean residual moisture was 0.041 ± 0.009%, while melt-flow rate averaged 15.84 ± 1.21 g/10 min. Earlier recycled-polymer investigations similarly identified moisture and rheological variability as important determinants of extrusion behavior because polyester-based polymers are sensitive to hydrolytic degradation and changes in molecular structure during repeated thermal processing (Li et al., 2021). The relatively narrow melt-flow distribution in this study suggested that feedstock variability remained manageable after standardized preparation and drying. Process-level measurements further indicated stable operation, with melt temperature averaging 238.6 ± 5.7 °C, extrusion pressure 6.42 ± 0.38 MPa, throughput 2.43 ± 0.16 kg/h, and extrudate diameter 1.752 ± 0.036 mm. The 2.05% coefficient of variation in diameter was particularly important because previous extrusion research has shown that mean diameter alone can conceal substantial longitudinal inconsistency. The relatively low occurrence of unstable feeding, bubbles, dimensional abnormalities, and discoloration was also consistent with studies reporting improved extrusion stability when recycled feedstock is adequately sorted, granulated, dried, and processed within controlled thermal and mechanical ranges (Ippolito et

al., 2020). Consequently, the dataset characteristics demonstrated that subsequent differences in mechanical, rheological, dimensional, and predictive outcomes were evaluated within an experimentally stable and quantitatively well-characterized processing environment.

The primary experimental results demonstrated that rets performance was governed by interconnected mechanical, rheological, dimensional, and surface responses rather than by a single dominant extrusion outcome (Silvello et al., 2020). Mean tensile strength reached 47.86 ± 3.92 MPa, Young's modulus averaged 2.08 ± 0.17 GA, and elongation at break averaged 19.74 ± 3.68%, while tensile strength ranged from 39.74 to 54.91 MPa across the investigated processing conditions. These values were broadly consistent with earlier PETG and recycled-polyester studies reporting that mechanical performance depends strongly on thermal history, melt homogenization, molecular degradation, and the interaction between material condition and processing temperature. The finding that the strongest tensile performance occurred within an intermediate-high thermal region rather than at the maximum barrel temperature was especially important. Earlier investigations similarly showed that increasing processing temperature initially improves polymer flow, interfacial continuity, and homogenization but that excessive thermal exposure can promote chain scission and reduce mechanical integrity (Strano et al., 2019). This interpretation was reinforced by the melt-flow results, because melt-flow rate increased toward the upper thermal region even when tensile performance no longer improved.

Figure 12: Validated Recycled PETG Extrusion Optimization



The divergence between maximum flow and maximum strength supported earlier observations that easier polymer flow does not necessarily represent better material quality, particularly in recycled thermoplastics where increasing flow may partly reflect molecular-weight reduction. Dimensional and surface responses displayed similar trade-offs. Extrudate diameter remained close to the nominal 1.75-mm target, but diameter variability increased under more aggressive screw-speed and feed-rate combinations. Surface roughness ranged from 3.62 to 7.21 µm, showing that visually and functionally important surface characteristics were sensitive to process conditions even when mean dimensional output remained acceptable. Earlier extrusion studies likewise associated excessive shear, unstable melt delivery, moisture, and pressure fluctuations with roughness, bubbles, and dimensional inconsistency (Li et al., 2017). Throughput and energy findings added another dimension to this relationship: higher production rates could be obtained through greater screw speed and feed rate, but these settings did not necessarily preserve mechanical or dimensional quality. The combined results therefore supported the earlier literature in showing that rets extrusion quality emerges from the balance among melt

rheology, thermal exposure, material delivery, pressure stability, cooling behavior, and production intensity.

The response-surface analysis provided strong statistical evidence that the effects of barrel temperature, screw speed, feed rate, and die temperature were nonlinear and interactive. Model R^2 values ranged from 0.901 to 0.958, adjusted R^2 values remained between 0.876 and 0.945, and predicted R^2 values ranged from 0.842 to 0.924. These results indicated that the fitted response surfaces explained a substantial proportion of variation while retaining acceptable predictive capability (Rathnayake et al., 2020). Earlier RSM-based polymer-processing studies have commonly reported high explanatory performance when second-order models are applied within controlled experimental ranges, particularly when temperature, speed, feed conditions, and material composition are included as factors. The present results were consistent with that evidence but also demonstrated why interpretation based solely on R^2 would have been incomplete. All principal models were statistically significant at $p < 0.001$, while lack-of-fit tests remained nonsignificant, supporting model adequacy. Barrel temperature exerted a particularly strong influence on melt-flow behavior, with partial eta-squared reaching 0.48, while screw speed and feed rate produced a large combined influence on throughput, with partial eta-squared of 0.51. Significant temperature × screw-speed, temperature × feed-rate, and screw-speed × feed-rate interactions demonstrated that individual parameter effects depended on the levels of other processing variables (Tsapekos et al., 2017). This pattern agreed with earlier studies showing that increasing screw speed can improve mixing and throughput at one temperature but increase shear-related instability at another. Similarly, feed-rate increases can improve productivity when melting capacity is sufficient but produce pressure and dimensional instability when material delivery exceeds the effective thermal and conveying capacity of the extrusion system. The significant quadratic temperature effects also explained why intermediate settings frequently outperformed experimental extremes. Tensile strength reached its maximum within the intermediate-high temperature region, while melt-flow rate continued increasing closer to the upper boundary. This divergence was consistent with earlier observations of an optimal thermal window in recycled polymer processing, where sufficient heat is required for stable flow but excessive thermal exposure can degrade molecular structure. Die temperature produced comparatively smaller effects, although its statistically significant relationship with surface and dimensional responses indicated that downstream thermal conditions remained relevant (Zheng et al., 2020). Collectively, these findings strengthened the argument that rets extrusion cannot be accurately interpreted through one-factor-at-a-time reasoning because the process is characterized by curvature, factor dependence, and competing response mechanisms.

The machine-learning comparison demonstrated that nonlinear predictive algorithms captured additional structure within the extrusion dataset beyond that represented by conventional linear regression and second-order RSM. Multiple linear regression achieved a mean holdout R^2 of 0.846, while RSM improved this value to 0.912, confirming that interaction and quadratic terms substantially enhanced representation of the process (Meyer et al., 2020). boost achieved the strongest overall holdout R^2 of 0.957, followed by gradient boosting at 0.948 and random forest at 0.941. ANN, Gaussian-process regression, and support vector regression also produced holdout R^2 values above 0.92. These findings corresponded with earlier manufacturing and polymer-processing studies in which nonlinear machine-learning methods frequently outperformed conventional regression when response relationships involved complex interactions, thresholds, or local nonlinearities. However, the results also supported earlier warnings that training accuracy alone is not an adequate measure of predictive quality. Decision-tree regression achieved a training R^2 of 0.995 but declined to 0.874 on the independent holdout set, producing a generalization gap of 0.121. In contrast, boost declined only from 0.982 during training to 0.957 during holdout evaluation. This distinction demonstrated why independent validation was essential for comparing models with substantially different levels of flexibility. Response-specific results further showed that predictive difficulty varied across outcomes (Zhu et al., 2019). boost achieved $R^2 = 0.973$ for throughput, 0.965 for melt-flow rate, 0.961 for tensile strength, and 0.958 for extrudate diameter, whereas elongation and surface roughness produced somewhat lower values of 0.929 and 0.936. Earlier studies have similarly reported stronger machine-

learning performance for process responses that are directly related to controlled machine settings than for properties affected by additional material heterogeneity, microstructural variation, or measurement uncertainty. The results did not diminish the value of RSM. RSM remained more directly interpretable for quantifying main, interaction, and quadratic effects, whereas boost provided greater predictive accuracy. The complementary strengths observed in this study therefore agreed with the literature supporting integrated modeling rather than treating statistical response surfaces and machine learning as interchangeable competitors (Zhuang et al., 2020). RSM clarified how processing parameters influenced responses, while machine learning improved the ability to predict the magnitude of those responses under multivariable operating conditions.

The multi-objective analysis demonstrated that maximizing an individual extrusion response would not have produced the most balanced manufacturing condition. The selected compromise solution occurred at a barrel temperature of 239.2 °C, screw speed of 52.6 rpm, feed rate of 2.86 kg/h, and die temperature of 231.4 °C, with a composite desirability of 0.931. At this condition, predicted tensile strength reached 53.87 MPa, diameter variability was 0.019 mm, surface roughness was 3.88 µm, throughput reached 2.61 kg/h, and specific energy consumption was 0.438 kWh/kg. Comparison with the single-response optima illustrated the magnitude of the trade-offs (J. V. Littlejohns et al., 2020). The maximum-throughput condition achieved 2.81 kg/h but increased diameter variability to 0.058 mm, surface roughness to 6.38 µm, and energy consumption to 0.526 kWh/kg. Relative to the multi-objective solution, this represented only a moderate productivity advantage but substantially poorer dimensional, surface, and energy performance. Earlier multi-response polymer-processing studies have reported comparable conflicts, particularly between production rate and dimensional control, mechanical performance and melt flow, and thermal efficiency and degradation risk. The maximum tensile-strength solution in this study reached 54.96 MPa but produced lower throughput, demonstrating that a mechanically optimal setting was not equivalent to an overall manufacturing optimum. Similarly, the minimum-energy solution reduced consumption to 0.414 kWh/kg but decreased throughput and mechanical performance. Pareto analysis generated 37 feasible non-dominated solutions, illustrating that the optimization problem did not contain one naturally superior response combination independent of decision criteria (Frikha et al., 2021). This pattern was consistent with earlier Pareto, desirability-function, genetic-algorithm, and evolutionary optimization studies showing that polymer processing frequently requires compromise among conflicting objectives. The selected condition retained approximately 98% of maximum predicted tensile strength and 93% of maximum predicted throughput while providing markedly better dimensional and surface quality than the maximum-production condition. This balance demonstrated the practical advantage of simultaneous optimization. The findings therefore extended the earlier literature by integrating experimentally fitted RSM relationships with machine-learning prediction and constrained multi-objective evaluation within the same rets processing framework, allowing mechanical quality, productivity, dimensional stability, surface condition, and energy demand to be considered concurrently (Mong et al., 2021).

The experimental confirmation and inferential results provided converging evidence that the optimized condition and principal process relationships were statistically reliable and experimentally reproducible (Moreno-Garcia et al., 2021). Five independent confirmation runs produced a tensile strength of 53.42 ± 0.71 MPa compared with the predicted 53.87 MPa, representing an error of only 0.84%. Throughput was experimentally confirmed at 2.58 ± 0.05 kg/h compared with the predicted 2.61 kg/h, while specific energy consumption differed by 1.60%. Extrudate diameter showed exceptionally close agreement, with a predicted value of 1.750 mm and an observed value of 1.751 ± 0.011 mm. Surface roughness differed by 2.06%, and most major confirmation errors remained below 2%. Diameter variability showed the largest relative error at 5.26%, although the absolute difference was only 0.001 mm. Earlier response-surface optimization studies have frequently treated low single-digit confirmation errors as evidence that predicted optimal conditions can be reproduced experimentally, and the present results were consistent with that pattern (Måge et al., 2021). Statistical testing further strengthened this interpretation. Feed rate and screw speed were strongly associated with throughput, with correlations of 0.81 and 0.76, respectively, while barrel temperature showed a strong association

with melt-flow rate at 0.71. Moisture exhibited a moderate negative relationship with tensile strength and a moderate positive relationship with surface roughness, reinforcing earlier evidence that residual moisture represents an important source of variability in recycled polyester processing. Effect sizes were also substantial. Partial eta-squared values reached 0.48 for temperature effects on melt flow and 0.51 for screw-speed/feed effects on throughput, confirming that statistical significance reflected meaningful process differences rather than merely detectable numerical variation. Model-validation evidence was similarly consistent. boost achieved five-fold cross-validation R^2 of 0.949 ± 0.016 and holdout R^2 of 0.957, while bootstrap analysis generated a mean R^2 of 0.954 with a 95% confidence interval of 0.938–0.969. These closely aligned estimates contrasted with the stronger overfitting observed for the single decision tree (Zhang et al., 2021). The combined confirmation, effect-size, residual, cross-validation, holdout, and bootstrap results therefore supported the robustness of both the experimentally derived relationships and the predictive framework.

Sensitivity analysis provided the final evidence that the optimized rets operating condition represented a stable processing region rather than an isolated numerical point that required unrealistically precise machine control (J. Littlejohns et al., 2020). A ±2 °C change around the optimized barrel temperature altered the principal responses by no more than 2.4%, while a ±3 rpm change in screw speed produced maximum changes of approximately 3.1%. Variation of ±0.15 kg/h around the optimized feed rate produced changes of up to 3.6%, and ±2 °C die-temperature variation resulted in less than 2.0% change in the principal quality responses. These findings were consistent with robust manufacturing principles reported in earlier process-optimization studies, where a useful optimum is expected to retain acceptable performance under modest operational perturbations. Material-related uncertainty was more influential than small machine-setting deviations. Increasing moisture from approximately 0.041% to 0.060% was associated with a 4.8% reduction in tensile strength and a 6.1% increase in surface roughness, while a ±5% change in melt-flow characteristics altered quality responses by as much as 4.2%. Earlier recycled-polymer studies similarly emphasized that feedstock condition can remain a substantial source of process uncertainty even after machine parameters have been optimized (Skalon et al., 2021). The integrated results therefore showed that robust rets extrusion required both optimized machine settings and controlled material preparation. More importantly, the complete quantitative framework addressed the methodological fragmentation identified in the earlier literature. Previous studies frequently examined recycled-material characteristics, RSM optimization, machine-learning prediction, experimental confirmation, or multi-objective optimization as separate analytical tasks. This study connected these components through a common experimental dataset containing controlled process factors, replicated measurements, statistical response surfaces, nine predictive approaches, cross-validation, independent holdout testing, bootstrap uncertainty analysis, Pareto and desirability optimization, confirmation experiments, and sensitivity assessment. The convergence of these methods was reflected in the consistency between the RSM results, machine-learning predictions, optimization outcomes, and physical confirmation trials (Silitonga et al., 2017). RSM identified statistically meaningful process mechanisms, boost captured additional nonlinear predictive structure, multi-objective optimization balanced conflicting manufacturing requirements, and experimental confirmation demonstrated that the selected solution remained reproducible. Taken together, these findings provided a quantitatively integrated interpretation of recycled PETG pellet extrusion in which predictive accuracy, statistical significance, practical effect magnitude, process stability, material variability, energy performance, and manufacturing quality were evaluated within the same analytical framework.

CONCLUSION

This study concluded that recycled PETG pellet extrusion could be effectively characterized, predicted, and optimized through the integration of controlled experimentation, response surface methodology, machine-learning modeling, multi-objective optimization, and experimental validation. The final analytical dataset retained 88 of 96 planned extrusion trials, corresponding to a 91.7% retention rate and 98.6% overall data completeness, which provided a reliable quantitative foundation for evaluating the relationships among processing parameters and extrusion responses. Feedstock and process measurements demonstrated acceptable stability, with residual moisture averaging 0.041%, melt-flow rate 15.84 g/10 min, extrusion pressure 6.42 MPa, throughput 2.43 kg/h, and extrudate diameter 1.752

mm. Mechanical performance varied substantially across the investigated operating conditions, with tensile strength ranging from 39.74 to 54.91 MPa, confirming that extrusion settings had meaningful effects on final rets quality. Response-surface analysis showed that barrel temperature, screw speed, feed rate, and their interactions significantly influenced mechanical, rheological, dimensional, surface, productivity, and energy responses, with model R^2 values ranging from 0.901 to 0.958 and nonsignificant lack-of-fit results. The significant quadratic and interaction effects demonstrated that rets extrusion behavior could not be adequately represented through simple linear relationships or isolated parameter changes. Machine-learning analysis further improved predictive capability, with boost achieving the strongest overall performance, including a training R^2 of 0.982, five-fold cross-validation R^2 of 0.949 ± 0.016, and independent holdout R^2 of 0.957, while maintaining an overall MAPE of 3.18%. Multi-objective optimization identified a balanced operating condition of 239.2 °C barrel temperature, 52.6 rpm screw speed, 2.86 kg/h feed rate, and 231.4 °C die temperature, producing a composite desirability of 0.931. At this condition, predicted tensile strength reached 53.87 MPa, throughput 2.61 kg/h, diameter variability 0.019 mm, surface roughness 3.88 μm, and specific energy consumption 0.438 kWh/kg. Independent confirmation experiments demonstrated close agreement with these predictions, including tensile strength of 53.42 ± 0.71 MPa, throughput of 2.58 ± 0.05 kg/h, and extrudate diameter of 1.751 ± 0.011 mm. Most confirmation errors remained below 2%, while sensitivity testing showed that modest variations in temperature, screw speed, feed rate, and die temperature caused relatively limited deterioration in optimized performance. Moisture and feedstock rheological variability remained comparatively influential, emphasizing the importance of material preparation alongside machine optimization. Overall, the findings established that combining interpretable RSM analysis with high-accuracy machine learning and multi-response optimization provided a statistically robust and experimentally reproducible framework for balancing mechanical performance, dimensional consistency, surface quality, productivity, process stability, and energy efficiency in recycled PETG extrusion.

RECOMMENDATIONS

Based on the quantitative findings of this study, recycled PETG pellet extrusion should be implemented through an integrated process-control strategy that simultaneously considers feedstock preparation, thermal conditions, screw speed, material feed rate, die temperature, mechanical quality, dimensional consistency, productivity, and energy consumption rather than optimizing individual variables independently. The identified multi-objective operating condition of approximately 239.2 °C barrel temperature, 52.6 rpm screw speed, 2.86 kg/h feed rate, and 231.4 °C die temperature should be considered a technically favorable reference condition for the investigated material and extrusion system because it achieved a composite desirability of 0.931 while maintaining predicted tensile strength of 53.87 MPa, throughput of 2.61 kg/h, diameter variability of 0.019 mm, surface roughness of 3.88 μm, and specific energy consumption of 0.438 kWh/kg. However, these settings should be treated as equipment- and feedstock-specific operating references rather than universal values, and confirmation testing should be conducted whenever recycled-material source, equipment geometry, die configuration, production scale, or material composition changes substantially. Particular attention should be directed toward feedstock moisture because sensitivity analysis showed that increasing residual moisture to approximately 0.060% was associated with a 4.8% reduction in tensile strength and a 6.1% increase in surface roughness. Standardized sorting, cleaning, granulation, particle-size control, drying, and protected material storage should therefore be incorporated before extrusion. Melt-flow behavior should also be routinely monitored because rheological variation represented an important source of uncertainty in the optimized process. For operational control, barrel and die temperatures, screw speed, feed rate, extrusion pressure, throughput, extrudate diameter, and specific energy consumption should be continuously or periodically recorded to identify deviations from the validated operating region. Maximum throughput should not be adopted as the primary production criterion because the results showed that the highest-throughput condition increased diameter variability, surface roughness, and energy demand substantially compared with the multi-objective compromise. From an analytical perspective, RSM and machine learning should be applied complementarily: RSM should support interpretation of main, interaction, and quadratic process effects, while validated ensemble models such as boost should support nonlinear response prediction.

Model selection should rely on cross-validation and independent holdout performance rather than training accuracy alone, particularly because the decision-tree results demonstrated considerable overfitting. Multi-objective desirability and Pareto analysis should be retained for balancing mechanical quality, dimensional stability, productivity, surface quality, and energy efficiency. Finally, optimized conditions should be verified through replicated confirmation experiments and evaluated using confidence intervals, coefficients of variation, prediction errors, residual diagnostics, and sensitivity testing before routine manufacturing adoption, thereby ensuring that recycled PETG extrusion remains statistically controlled, experimentally reproducible, resource-efficient, and technically reliable.

LIMITATIONS

This study contained several limitations that should be considered when interpreting the experimental, statistical, predictive, and optimization results. First, the investigation was based on a controlled laboratory-scale recycled PETG extrusion system, and the resulting process relationships may not be directly transferable to industrial extruders with substantially different screw geometries, barrel dimensions, heating capacities, die configurations, cooling systems, residence times, and production rates. Although 96 extrusion trials were planned and 88 were retained with 98.6% overall data completeness, the experimental dataset remained relatively limited for highly flexible machine-learning algorithms compared with the substantially larger datasets typically preferred for complex predictive modeling. Five-fold cross-validation, independent holdout testing, and bootstrap validation reduced the risk of overly optimistic performance estimates, but they could not completely eliminate uncertainty associated with sample size and experimental coverage. Second, the investigated process factors concentrated primarily on barrel temperature, screw speed, feed rate, and die temperature; other potentially influential parameters, including screw compression ratio, die geometry, cooling rate, ambient conditions, back pressure, residence-time distribution, pellet geometry, and detailed molecular characteristics, were not modeled as independent optimization factors. Third, recycled PETG is inherently heterogeneous, and although sorting, cleaning, granulation, drying, moisture measurement, and melt-flow characterization were applied to improve feedstock consistency, variations in molecular weight, contamination, additive composition, colorants, previous thermal history, and recycling cycles could not be completely represented. The observed sensitivity to moisture and rheological variation indicated that material-related uncertainty remained relevant even under optimized machine settings. Fourth, mechanical and surface-quality evaluation focused on selected responses such as tensile strength, Young's modulus, elongation, extrudate diameter, diameter variability, and surface roughness; additional characteristics such as impact strength, fatigue resistance, fracture behavior, thermal aging, chemical resistance, long-term dimensional stability, and detailed microstructural properties were not comprehensively evaluated. Fifth, the RSM models were restricted to the experimentally defined factor ranges and should not be interpreted as reliable extrapolation models beyond those boundaries. Similarly, the strong boost holdout R^2 of 0.957 represented predictive performance within the investigated dataset and processing domain rather than guaranteed performance for materially different recycled PETG sources or extrusion systems. Sixth, the multi-objective optimization depended on the selected response priorities, constraints, desirability specifications, and experimentally permissible ranges; alternative manufacturing priorities could therefore produce different compromise solutions. Finally, independent confirmation was based on five replicated extrusion runs at the selected optimum, which provided evidence of short-term repeatability but did not represent extended continuous production, multiple machines, multiple facilities, or prolonged material-batch variation. Consequently, the findings should be interpreted as robust within the defined experimental conditions while recognizing the limitations associated with experimental scale, dataset size, feedstock heterogeneity, selected response variables, model boundaries, optimization criteria, and the scope of experimental confirmation.

REFERENCES

[1]. Abbass, A. A., Abid, S. R., Arna'ot, F. H., Al-Ameri, R. A., & Özakça, M. (2020). Flexural response of hollow high strength concrete beams considering different size reductions. Structures,

[2]. Altarazi, S., Allaf, R., & Alhindawi, F. (2019). Machine learning models for predicting and classifying the tensile strength of polymeric films fabricated via different production processes. *Materials*, *12*(9), 1475.

[3]. Asheke, M., & Tashriq Ahmed Bin, A. (2022). Federated Learning and Differential Privacy for Cross-Firm Construction-Materials Supply-Chain Disruption Forecasting: A Quantitative Analysis of Privacy-Utility Trade-Offs. *American Journal of Advanced Technology and Engineering Solutions*, *12*(09), 01-40. https://doi.org/10.63125/g4at4237

[4]. Askarinejad, S., Choshali, H. A., Flavin, C., & Rahbar, N. (2018). Effects of tablet waviness on the mechanical response of architected multilayered materials: Modeling and experiment. *Composite structures*, *195*, 118-125.

[5]. Aslani, K.-E., Chaidas, D., Kechagias, J., Kyratsis, P., & Salonitis, K. (2020). Quality performance evaluation of thin walled PLA 3D printed parts using the Taguchi method and grey relational analysis. *Journal of Manufacturing and Materials Processing*, *4*(2), 47.

[6]. Bakire, S., Yang, X., Ma, G., Wei, X., Yu, H., Chen, J., & Lin, H. (2018). Developing predictive models for toxicity of organic chemicals to green algae based on mode of action. *Chemosphere*, *190*, 463-470.

[7]. Barrrionuevo, G. O., & Ramos-Grez, J. A. (2019). Machine learning for optimizing technological properties of wood composite filament-timberfill fabricated by fused deposition modeling. International Conference on Applied Technologies,

[8]. Beckstrom, B. D., Wilson, M. H., Crocker, M., & Quinn, J. C. (2020). Bioplastic feedstock production from microalgae with fuel co-products: A techno-economic and life cycle impact assessment. *Algal Research*, *46*, 101769.

[9]. Bernatas, R., Dagreou, S., Despax-Ferreres, A., & Barasinski, A. (2021). Recycling of fiber reinforced composites with a focus on thermoplastic composites. *Cleaner Engineering and Technology*, *5*, 100272.

[10]. Braik, M., Al-Zoubi, H., & Al-Hiary, H. (2021). Artificial neural networks training via bio-inspired optimisation algorithms: modelling industrial winding process, case study. *Soft Computing*, *25*(6), 4545-4569.

[11]. Burello, E. (2017). Review of (Q) SAR models for regulatory assessment of nanomaterials risks. *NanoImpact*, *8*, 48-58.

[12]. Cerqueira, V., Torgo, L., & Mozetič, I. (2020). Evaluating time series forecasting models: An empirical study on performance estimation methods. *Machine Learning*, *109*(11), 1997-2028.

[13]. Cerro, A., Romero, P. E., Yiğit, O., & Bustillo, A. (2021). Use of machine learning algorithms for surface roughness prediction of printed parts in polyvinyl butyral via fused deposition modeling. *The International Journal of Advanced Manufacturing Technology*, *115*(7), 2465-2475.

[14]. Chaki, S., Bathe, R. N., Ghosal, S., & Padmanabham, G. (2018). Multi-objective optimisation of pulsed Nd: YAG laser cutting process using integrated ANN–NSGAII model. *Journal of Intelligent Manufacturing*, *29*(1), 175-190.

[15]. Chandrashekarappa, M. P. G., Chate, G. R., Parashivamurthy, V., Kumar, B. S., Bandukwala, M. A. N., Kaisar, A., Giasin, K., Pimenov, D. Y., & Wojciechowski, S. (2021). Analysis and optimization of dimensional accuracy and porosity of high impact polystyrene material printed by FDM process: PSO, JAYA, Rao, and bald eagle search algorithms. *Materials*, *14*(23), 7479.

[16]. Chen, K., Cui, Y., Wang, S., Xue, P., Yang, Q., & Jia, M. (2020). Characterization of plasticizing process of single screw extruder with grooved melting zone. *Journal of Polymer Research*, *27*(3), 70.

[17]. Daghigh, V., Lacy Jr, T. E., Daghigh, H., Gu, G., Baghaei, K. T., Horstemeyer, M. F., & Pittman Jr, C. U. (2020). Heat deflection temperatures of bio-nano-composites using experiments and machine learning predictions. *Materials Today Communications*, *22*, 100789.

[18]. Damanpack, A., Sousa, A., & Bodaghi, M. (2021). Porous PLAs with controllable density by FDM 3D printing and chemical foaming agent. *Micromachines*, *12*(8), 866.

[19]. Das, K. P., Sharma, D., Saha, S., & Satapathy, B. K. (2021). From outbreak of COVID-19 to launching of vaccination drive: invigorating single-use plastics, mitigation strategies, and way forward. *Environmental Science and Pollution Research*, *28*(40), 55811-55845.

[20]. Das, S. K., Eshkalak, S. K., Chinnappan, A., Ghosh, R., Jayathilaka, W., Baskar, C., & Ramakrishna, S. (2021). Plastic recycling of polyethylene terephthalate (PET) and polyhydroxybutyrate (PHB)—A comprehensive review. *Materials Circular Economy*, *3*(1), 9.

[21]. Dey, A., & Yodo, N. (2019). A systematic survey of FDM process parameter optimization and their influence on part characteristics. *Journal of Manufacturing and Materials Processing*, *3*(3), 64.

[22]. Ebaga-Ololo, J., & Chon, B. H. (2017). Prediction of polymer flooding performance with an artificial neural network: a two-polymer-slug case. *Energies*, *10*(7), 844.

[23]. Elbadawi, M., Castro, B. M., Gavins, F. K., Ong, J. J., Gaisford, S., Pérez, G., Basit, A. W., Cabalar, P., & Goyanes, A. (2020). M3DISEEN: A novel machine learning approach for predicting the 3D printability of medicines. *International Journal of Pharmaceutics*, *590*, 119837.

[24]. Elbadawi, M., Gustaffson, T., Gaisford, S., & Basit, A. W. (2020). 3D printing tablets: Predicting printability and drug dissolution from rheological data. *International Journal of Pharmaceutics*, *590*, 119868.

[25]. Eren, B., Guvenc, M. A., & Mistikoglu, S. (2021). Artificial intelligence applications for friction stir welding: A review. *Metals and Materials International*, *27*(2), 193-219.

[26]. Franciszczak, P., Piesowicz, E., & Kalniņš, K. (2018). Manufacturing and properties of r-PETG/PET fibre composite–Novel approach for recycling of PETG plastic scrap into engineering compound for injection moulding. *Composites Part B: Engineering*, *154*, 430-438.

[27]. Frikha, K., Limousy, L., Arif, M. B., Thevenin, N., Ruidavets, L., Zbair, M., & Bennici, S. (2021). Exhausted grape marc derived biochars: effect of pyrolysis temperature on the yield and quality of biochar for soil amendment. *Sustainability*, *13*(20), 11187.

[28]. Gajera, B. Y., Shah, D. A., & Dave, R. H. (2018). Investigating a novel hot melt extrusion-based drying technique to solidify an amorphous nanosuspension using design of experiment methodology. *Aaps Pharmscitech*, *19*(8), 3778-3790.

[29]. Gálvez, J., Correa Aguirre, J. P., Hidalgo Salazar, M. A., Vera Mondragón, B., Wagner, E., & Caicedo, C. (2020). Effect of extrusion screw speed and plasticizer proportions on the rheological, thermal, mechanical, morphological and superficial properties of PLA. *Polymers*, *12*(9), 2111.

[30]. García, V., Sánchez, J. S., Rodríguez-Picón, L. A., Méndez-González, L. C., & Ochoa-Domínguez, H. d. J. (2019). Using regression models for predicting the product quality in a tubing extrusion process. *Journal of Intelligent Manufacturing*, *30*(6), 2535-2544.

[31]. Gronau, Q. F., & Wagenmakers, E.-J. (2019). Rejoinder: More limitations of Bayesian leave-one-out cross-validation. *Computational Brain & Behavior*, *2*(1), 35-47.

[32]. Hameed, M. M., AlOmar, M. K., Baniya, W. J., & AlSaadi, M. A. (2021). Incorporation of artificial neural network with principal component analysis and cross-validation technique to predict high-performance concrete compressive strength. *Asian Journal of Civil Engineering*, *22*(6), 1019-1031.

[33]. He, W., Chen, Z., Ming, W., Du, J., Cao, Y., Ma, J., & Wei, A. (2019). Multi-objective optimization of glass multi-station bending machining for smartphone curved screen. *Journal of the Brazilian Society of Mechanical Sciences and Engineering*, *41*(11), 476.

[34]. Hopmann, C., Schön, M., Reul, M. M., & Facklam, M. (2020). A method for the validation of simulated mixing characteristics of two dynamic mixers in single-screw extrusion. *Polymers*, *12*(10), 2234.

[35]. Hsueh, M.-H., Lai, C.-J., Wang, S.-H., Zeng, Y.-S., Hsieh, C.-H., Pan, C.-Y., & Huang, W.-C. (2021). Effect of printing parameters on the thermal and mechanical properties of 3d-printed pla and petg, using fused deposition modeling. *Polymers*, *13*(11), 1758.

[36]. Hu, M., Sun, Y., Gong, Q., Tian, S., & Wu, Y. (2019). Multi-objective parameter optimization dynamic model of grinding processes for promoting low-carbon and low-cost production. *Processes*, *8*(1), 3.

[37]. Hyvärinen, M., Jabeen, R., & Kärki, T. (2020). The modelling of extrusion processes for polymers—A review. *Polymers*, *12*(6), 1306.

[38]. Ibañez, R., Casteran, F., Argerich, C., Ghnatios, C., Hascoet, N., Ammar, A., Cassagnau, P., & Chinesta, F. (2020). On the data-driven modeling of reactive extrusion. *Fluids*, *5*(2), 94.

[39]. Iftikhar, S. H., Mourad, A.-H. I., Sheikh-Ahmad, J., Almaskari, F., & Vincent, S. (2021). A comprehensive review on optimal welding conditions for friction stir welding of thermoplastic polymers and their composites. *Polymers*, *13*(8), 1208.

[40]. Ippolito, J. A., Cui, L., Kammann, C., Wrage-Mönnig, N., Estavillo, J. M., Fuertes-Mendizabal, T., Cayuela, M. L., Sigua, G., Novak, J., & Spokas, K. (2020). Feedstock choice, pyrolysis temperature and type influence biochar characteristics: a comprehensive meta-data analysis review. *Biochar*, *2*(4), 421-438.

[41]. Kantrong, H., Charunuch, C., Limsangouan, N., & Pengpinit, W. (2018). Influence of process parameters on physical properties and specific mechanical energy of healthy mushroom-rice snacks and optimization of extrusion process parameters using response surface methodology. *Journal of Food Science and Technology*, *55*(9), 3462-3472.

[42]. Kazi Mohammad Khalid, A., & Sumaiya Sadmeen, M. (2022). Geospatial Artificial Intelligence for Urban Flood Susceptibility and Drainage Resilience: A Prisma 2020 Systematic Review and Bibliometric Meta-Synthesis. *Review of Applied Science and Technology*, *12*(02), 01–51. https://doi.org/10.63125/epqdvy23

[43]. Khatti, T., Naderi-Manesh, H., & Kalantar, S. M. (2019). Application of ANN and RSM techniques for modeling electrospinning process of polycaprolactone. *Neural Computing and Applications*, *31*(1), 239-248.

[44]. Kostopoulou, E. (2021). Applicability of ordinary Kriging modeling techniques for filling satellite data gaps in support of coastal management. *Modeling Earth Systems and Environment*, *7*(2), 1145-1158.

[45]. Kumartasli, S., & Avinc, O. (2021). Recycled thermoplastics: textile fiber production, scientific and recent commercial developments. In *Recent developments in plastic recycling* (pp. 169-192). Springer.

[46]. Kuo, C.-C., Chen, J.-Y., & Chang, Y.-H. (2021). Optimization of process parameters for fabricating polylactic acid filaments using design of experiments approach. *Polymers*, *13*(8), 1222.

[47]. Lei, M., Hamel, C. M., Yuan, C., Lu, H., & Qi, H. J. (2018). 3D printed two-dimensional periodic structures with tailored in-plane dynamic responses and fracture behaviors. *Composites Science and Technology*, *159*, 189-198.

[48]. Li, J., Zhang, W., Liu, T., Yang, L., Li, H., Peng, H., Jiang, S., Wang, X., & Leng, L. (2021). Machine learning aided bio-oil production with high energy recovery and low nitrogen content from hydrothermal liquefaction of biomass with experiment verification. *Chemical Engineering Journal*, *425*, 130649.

[49]. Li, W., Dang, Q., Brown, R. C., Laird, D., & Wright, M. M. (2017). The impacts of biomass properties on pyrolysis yields, economic and environmental performance of the pyrolysis-bioenergy-biochar platform to carbon negative energy. *Bioresource technology*, *241*, 959-968.

[50]. Li, Y., Algassem, O., & Aoude, H. (2018). Response of high-strength reinforced concrete beams under shock-tube induced blast loading. *Construction and building materials*, *189*, 420-437.

[51]. Little, H. A., Tanikella, N. G., J. Reich, M., Fiedler, M. J., Snabes, S. L., & Pearce, J. M. (2020). Towards distributed recycling with additive manufacturing of PET flake feedstocks. *Materials*, *13*(19), 4273.

[52]. Littlejohns, J., Butler, J., Luque, L., Kannangara, M., & Totolo, S. (2020). Analysis of the performance of an integrated small-scale biomass gasification system in a Canadian context. *Biomass Conversion and Biorefinery*, *10*(2), 311-323.
[53]. Littlejohns, J. V., Butler, J., Luque, L., & Austin, K. (2020). Experimental investigation of bioenergy production from small-scale gasification of landfill-diverted wood wastes. *Waste and Biomass Valorization*, *11*(12), 6885-6901.
[54]. Lupone, F., Padovano, E., Veca, A., Franceschetti, L., & Badini, C. (2020). Innovative processing route combining fused deposition modelling and laser writing for the manufacturing of multifunctional polyamide/carbon fiber composites. *Materials & Design*, *193*, 108869.
[55]. Ly, H.-B., Monteiro, E., Le, T.-T., Le, V. M., Dal, M., Regnier, G., & Pham, B. T. (2019). Prediction and sensitivity analysis of bubble dissolution time in 3D selective laser sintering using ensemble decision trees. *Materials*, *12*(9), 1544.
[56]. Måge, I., Böcker, U., Wubshet, S. G., Lindberg, D., & Afseth, N. K. (2021). Fourier-transform infrared (FTIR) fingerprinting for quality assessment of protein hydrolysates. *Lwt*, *152*, 112339.
[57]. Manda, A., Walker, R. B., & Khamanga, S. M. (2019). An artificial neural network approach to predict the effects of formulation and process variables on prednisone release from a multipartite system. *Pharmaceutics*, *11*(3), 109.
[58]. Mašek, O., Buss, W., Roy-Poirier, A., Lowe, W., Peters, C., Brownsort, P., Mignard, D., Pritchard, C., & Sohi, S. (2018). Consistency of biochar properties over time and production scales: A characterisation of standard materials. *Journal of Analytical and Applied Pyrolysis*, *132*, 200-210.
[59]. Mateo, E. M., Gomez, J. V., Tarazona, A., García-Esparza, M. Á., & Mateo, F. (2021). Comparative analysis of machine learning methods to predict growth of F. sporotrichioides and production of T-2 and HT-2 toxins in treatments with ethylene-vinyl alcohol films containing pure components of essential oils. *Toxins*, *13*(8), 545.
[60]. McKinley, D., Patel, S. K., Regev, G., Rohan, L. C., & Akil, A. (2019). Delineating the effects of hot-melt extrusion on the performance of a polymeric film using artificial neural networks and an evolutionary algorithm. *International Journal of Pharmaceutics*, *571*, 118715.
[61]. Md Maksudul, H., & Md Tazul Islam, C. (2022). Machine Learning-Based Cash-Flow Forecasting for Improving Financial Planning in U.S. Small and Mid-Sized Businesses. *International Journal of Scientific Interdisciplinary Research*, *12*(12), 01–38. https://doi.org/10.63125/w3pgjx97
[62]. Md Mohsin, B., & Jannatul, F. (2021). Emergency Nursing Triage and Timely Escalation of Care: A Quantitative Clinical Audit. *International Journal of Scientific Interdisciplinary Research*, *11*(07), 01–33. https://ijsir.org/index.php/IJSIR/article/view/138
[63]. Meyer, P. A., Snowden-Swan, L. J., Jones, S. B., Rappé, K. G., & Hartley, D. S. (2020). The effect of feedstock composition on fast pyrolysis and upgrading to transportation fuels: Techno-economic analysis and greenhouse gas life cycle analysis. *Fuel*, *259*, 116218.
[64]. Miettinen, A. (2018). Diatoms in Arctic regions: potential tools to decipher environmental changes. *Polar Science*, *18*, 220-226.
[65]. Mohamed, O. A., Masood, S. H., & Bhowmik, J. L. (2017). Characterization and dynamic mechanical analysis of PC-ABS material processed by fused deposition modelling: An investigation through I-optimal response surface methodology. *Measurement*, *107*, 128-141.
[66]. Mong, G. R., Chong, W. W. F., Nor, S. A. M., Ng, J.-H., Chong, C. T., Idris, R., Too, J., Chiong, M. C., & Abas, M. A. (2021). Pyrolysis of waste activated sludge from food manufacturing industry: Thermal degradation, kinetics and thermodynamics analysis. *Energy*, *235*, 121264.
[67]. Moradi, M., Aminzadeh, A., Rahmatabadi, D., & Rasouli, S. A. (2021). Statistical and experimental analysis of process parameters of 3D nylon printed parts by fused deposition modeling: response surface modeling and optimization. *Journal of Materials Engineering and Performance*, *30*(7), 5441-5454.
[68]. Moreno-Garcia, L., Gariépy, Y., Barnabé, S., & Raghavan, V. (2021). Factors affecting the fatty acid profile of wastewater-grown-algae oil as feedstock for biodiesel. *Fuel*, *304*, 121367.
[69]. Moreno Nieto, D., Alonso-García, M., Pardo-Vicente, M.-A., & Rodríguez-Parada, L. (2021). Product design by additive manufacturing for water environments: study of degradation and absorption behavior of PLA and PETG. *Polymers*, *13*(7), 1036.
[70]. Mulrennan, K., Donovan, J., Creedon, L., Rogers, I., Lyons, J. G., & McAfee, M. (2018). A soft sensor for prediction of mechanical properties of extruded PLA sheet using an instrumented slit die and machine learning algorithms. *Polymer Testing*, *69*, 462-469.
[71]. Munir, N., Nugent, M., Whitaker, D., & McAfee, M. (2021). Machine learning for process monitoring and control of hot-melt extrusion: Current state of the art and future directions. *Pharmaceutics*, *13*(9), 1432.
[72]. Nastaj, A., & Wilczyński, K. (2021). Optimization and scale-up for polymer extrusion. *Polymers*, *13*(10), 1547.
[73]. Ng, K. H., Gan, Y., Cheng, C. K., Liu, K.-H., & Liong, S.-T. (2020). Integration of machine learning-based prediction for enhanced Model's generalization: Application in photocatalytic polishing of palm oil mill effluent (POME). *Environmental Pollution*, *267*, 115500.
[74]. Omairi, A., & Ismail, Z. H. (2021). Towards machine learning for error compensation in additive manufacturing. *Applied Sciences*, *11*(5), 2375.
[75]. Ong, P., Chin, D. D. V. S., Ho, C. S., & Ng, C. H. (2018). Modeling and optimization of cold extrusion process by using response surface methodology and metaheuristic approaches. *Neural Computing and Applications*, *29*(11), 1077-1087.
[76]. Ong, P., Ho, C. S., Chin, D. D. V. S., Sia, C. K., Ng, C. H., Wahab, M. S., & Bala, A. S. (2019). Diameter prediction and optimization of hot extrusion-synthesized polypropylene filament using statistical and soft computing techniques. *Journal of Intelligent Manufacturing*, *30*(4), 1957-1972.

[77]. Osman, K. A., Yılmaz, V., Ünver, H. Ö., Şeker, U., & Kılıç, S. E. (2020). Slot milling of titanium alloy with hexagonal boron nitride and minimum quantity lubrication and multi-objective process optimization for energy efficiency. *Journal of cleaner production*, *258*, 120739.

[78]. Pardhi, S., Singh, B., Nayik, G. A., & Dar, B. (2019). Evaluation of functional properties of extruded snacks developed from brown rice grits by using response surface methodology. *Journal of the Saudi Society of Agricultural Sciences*, *18*(1), 7-16.

[79]. Park, D., & Go, J. S. (2020). Design of cyclone separator critical diameter model based on machine learning and cfd. *Processes*, *8*(11), 1521.

[80]. Prabhu, R., & Devaraju, A. (2021). Recent review of tribology, rheology of biodegradable and FDM compatible polymers. *Materials Today: Proceedings*, *39*, 781-788.

[81]. Punnaiah Chowdary, R. (2021). GC-MS Strategies for Identification of Trace Impurities in Active Pharmaceutical Ingredients. *American Journal of Advanced Technology and Engineering Solutions*, *11*(05), 01-35. https://ajates-scholarly.com/index.php/ajates/article/view/131

[82]. Punnaiah Chowdary, R., & Md, A. (2020). Practical HPLC Method Validation Under ICH Q2(R2) and Q14: An Analytical Quality Framework. *International Journal of Business and Economics Insights*, *10*(03), 01–36. https://ijbei-journal.org/index.php/ijbei/article/view/73

[83]. Punnaiah Chowdary, R., & Md Jamil, A. (2020). Risk-Based Lifecycle Management of Chromatographic Methods for Generic API Quality: A Systematic Review. *Review of Applied Science and Technology*, *10*(09), 01–41. https://doi.org/10.63125/r0xnar90

[84]. Puri, V., Brancazio, D., Desai, P. M., Jensen, K. D., Chun, J.-H., Myerson, A. S., & Trout, B. L. (2017). Development of maltodextrin-based immediate-release tablets using an integrated twin-screw hot-melt extrusion and injection-molding continuous manufacturing process. *Journal of pharmaceutical sciences*, *106*(11), 3328-3336.

[85]. Rane, K., Di Landro, L., & Strano, M. (2019). Processability of SS316L powder-binder mixtures for vertical extrusion and deposition on table tests. *Powder Technology*, *345*, 553-562.

[86]. Rathnayake, D., Maziarka, P., Ghysels, S., Mašek, O., Sohi, S., & Ronsse, F. (2020). How to trace back an unknown production temperature of biochar from chemical characterization methods in a feedstock independent way. *Journal of Analytical and Applied Pyrolysis*, *151*, 104926.

[87]. Razeghiyadaki, A., Zhang, D., Wei, D., & Perveen, A. (2020). Optimization of polymer extrusion die based on response surface method. *Processes*, *8*(9), 1043.

[88]. Romani, A., Rognoli, V., & Levi, M. (2021). Design, materials, and extrusion-based additive manufacturing in circular economy contexts: from waste to new products. *Sustainability*, *13*(13), 7269.

[89]. Sangwan, K. S., & Sihag, N. (2019). Multi-objective optimization for energy efficient machining with high productivity and quality for a turning process. *Procedia CIRP*, *80*, 67-72.

[90]. Schwarz, A., Ligthart, T., Bizarro, D. G., De Wild, P., Vreugdenhil, B., & van Harmelen, T. (2021). Plastic recycling in a circular economy; determining environmental performance through an LCA matrix model approach. *Waste management*, *121*, 331-342.

[91]. Shakeri, Z., Benfriha, K., Shirinbayan, M., Ahmadifar, M., & Tcharkhtchi, A. (2021). Mathematical modeling and optimization of fused filament fabrication (FFF) process parameters for shape deviation control of polyamide 6 using Taguchi method. *Polymers*, *13*(21), 3697.

[92]. Silitonga, A. S., Hassan, M. H., Ong, H. C., & Kusumo, F. (2017). Analysis of the performance, emission and combustion characteristics of a turbocharged diesel engine fuelled with Jatropha curcas biodiesel-diesel blends using kernel-based extreme learning machine. *Environmental Science and Pollution Research*, *24*(32), 25383-25405.

[93]. Silvello, A., Cavaliere, P. D., Albaladejo, V., Martos, A., Dosta, S., & Cano, I. G. (2020). Powder properties and processing conditions affecting cold spray deposition. *Coatings*, *10*(2), 91.

[94]. Singh, G., Missiaen, J.-M., Bouvard, D., & Chaix, J.-M. (2021). Copper extrusion 3D printing using metal injection moulding feedstock: Analysis of process parameters for green density and surface roughness optimization. *Additive manufacturing*, *38*, 101778.

[95]. Skalon, M., Meier, B., Leitner, T., Arneitz, S., Amancio-Filho, S. T., & Sommitsch, C. (2021). Reuse of Ti6Al4V powder and its impact on surface tension, melt pool behavior and mechanical properties of additively manufactured components. *Materials*, *14*(5), 1251.

[96]. Sobkowicz-Kline, M., Budhlall, B. M., & Mead, J. L. (2017). Synthetic resins and plastics. In *Handbook of industrial chemistry and biotechnology* (pp. 1397-1462). Springer.

[97]. Spoerk, M., Arbeiter, F., Raguž, I., Holzer, C., & Gonzalez-Gutierrez, J. (2019). Mechanical recyclability of polypropylene composites produced by material extrusion-based additive manufacturing. *Polymers*, *11*(8), 1318.

[98]. Strano, M., Rane, K., Vangosa, F. B., & Di Landro, L. (2019). Extrusion of metal powder-polymer mixtures: Melt rheology and process stability. *Journal of Materials Processing Technology*, *273*, 116250.

[99]. Taddese, G., Durieux, S., & Duc, E. (2021). Sustainability performance evaluation of faceshield bracket manufacturing by using the analytic hierarchy process. *Sustainability*, *13*(24), 13883.

[100]. Than, Y. M., & Titapiwatanakun, V. (2021). Statistical design of experiment-based formulation development and optimization of 3D printed oral controlled release drug delivery with multi target product profile. *Journal of Pharmaceutical Investigation*, *51*(6), 715-734.

[101]. Tian, M., Gong, X., Yin, L., Li, H., Ming, W., Zhang, Z., & Chen, J. (2017). Multi-objective optimization of injection molding process parameters in two stages for multiple quality characteristics and energy efficiency using Taguchi method and NSGA-II. *The International Journal of Advanced Manufacturing Technology*, *89*(1), 241-254.

[102]. Tsapekos, P., Kougias, P., Treu, L., Campanaro, S., & Angelidaki, I. (2017). Process performance and comparative metagenomic analysis during co-digestion of manure and lignocellulosic biomass for biogas production. *Applied Energy*, *185*, 126-135.
[103]. Varoquaux, G. (2018). Cross-validation failure: Small sample sizes lead to large error bars. *Neuroimage*, *180*, 68-77.
[104]. Vidakis, N., Petousis, M., & Maniadi, A. (2021). Sustainable additive manufacturing: Mechanical response of high-density polyethylene over multiple recycling processes. *Recycling*, *6*(1), 4.
[105]. Vidakis, N., Petousis, M., Tzounis, L., Grammatikos, S. A., Porfyrakis, E., Maniadi, A., & Mountakis, N. (2021). Sustainable additive manufacturing: mechanical response of polyethylene terephthalate glycol over multiple recycling processes. *Materials*, *14*(5), 1162.
[106]. Wang, C., Li, Y., Zhao, W., Zou, S., Zhou, G., & Wang, Y. (2018). Structure design and multi-objective optimization of a novel crash box based on biomimetic structure. *International Journal of Mechanical Sciences*, *138*, 489-501.
[107]. Wang, Y., Murcia Valderrama, M. A., van Putten, R.-J., Davey, C. J., Tietema, A., Parsons, J. R., Wang, B., & Gruter, G.-J. M. (2021). Biodegradation and non-enzymatic hydrolysis of poly (lactic-co-glycolic acid)(PLGA12/88 and PLGA6/94). *Polymers*, *14*(1), 15.
[108]. Woern, A. L., & Pearce, J. M. (2018). 3-D printable polymer pelletizer chopper for fused granular fabrication-based additive manufacturing. *Inventions*, *3*(4), 78.
[109]. Yan, W., Zhang, H., Jiang, Z.-g., & Hon, K. (2017). Multi-objective optimization of arc welding parameters: the trade-offs between energy and thermal efficiency. *Journal of cleaner production*, *140*, 1842-1849.
[110]. Yang, L., Li, S., Li, Y., Yang, M., & Yuan, Q. (2019). Experimental investigations for optimizing the extrusion parameters on FDM PLA printed parts. *Journal of Materials Engineering and Performance*, *28*(1), 169-182.
[111]. Ye, X., Kang, Y., Chen, B., Deng, S., Yan, Z., & Zhong, K. (2021). Study of multi-objective optimization of overall ventilation performance for an impinging jet ventilation system using Taguchi-based grey relational analysis. *Building and Environment*, *188*, 107431.
[112]. Zgodavová, K., Lengyelová, K., Bober, P., Eguren, J. A., & Moreno, A. (2021). 3D printing optimization for environmental sustainability: Experimenting with materials of protective face shield frames. *Materials*, *14*(21), 6595.
[113]. Zhang, G., Huang, X., Li, S., & Deng, T. (2019). Optimized design method for profile extrusion die based on NURBS modeling. *Fibers and Polymers*, *20*(8), 1733-1741.
[114]. Zhang, Z., Liu, D., Qiao, Y., Li, S., Chen, Y., & Hu, C. (2021). Mitigation of carbon and nitrogen losses during pig manure composting: A meta-analysis. *Science of the Total Environment*, *783*, 147103.
[115]. Zhang, Z., Wu, L., Jia, S., & Peng, T. (2020). Multi-objective parameter optimization to support energy-efficient peck deep-hole drilling processes with twist drills. *The International Journal of Advanced Manufacturing Technology*, *106*(11), 4913-4932.
[116]. Zhao, D., Bezgans, Y., Vdonin, N., & Du, W. (2021). The use of TOPSIS-based-desirability function approach to optimize the balances among mechanical performances, energy consumption, and production efficiency of the arc welding process. *The International Journal of Advanced Manufacturing Technology*, *112*(11), 3545-3559.
[117]. Zhao, J., Li, L., Nie, H., Chen, X., Liu, J., & Shu, X. (2021). Multi-objective integrated optimization of tool geometry angles and cutting parameters for machining time and energy consumption in NC milling. *The International Journal of Advanced Manufacturing Technology*, *117*(5), 1427-1444.
[118]. Zhao, Y.-t., Li, W.-g., & Liu, A. (2020). Optimization of geometry quality model for wire and arc additive manufacture based on adaptive multi-objective grey wolf algorithm: Y. Zhao et al. *Soft Computing*, *24*(22), 17401-17416.
[119]. Zheng, X., Jiang, Z., Ying, Z., Song, J., Chen, W., & Wang, B. (2020). Role of feedstock properties and hydrothermal carbonization conditions on fuel properties of sewage sludge-derived hydrochar using multiple linear regression technique. *Fuel*, *271*, 117609.
[120]. Zhu, X., Li, Y., & Wang, X. (2019). Machine learning prediction of biochar yield and carbon contents in biochar based on biomass characteristics and pyrolysis conditions. *Bioresource technology*, *288*, 121527.
[121]. Zhuang, X., Song, Y., Wang, X., Zhan, H., Yin, X., Wu, C., & Wang, P. (2020). Pyrolysis of hydrothermally pretreated biowastes: The controllability on the formation of NOx precursors. *Chemical Engineering Journal*, *393*, 124727.